R.T.
YILDIZ TECHNICAL UNIVERSITY
GRADUATE SCHOOL OF NATURAL AND APPLIED SCIENCES

DESIGN OF AN ULTRAWIDE BAND MICROSTRIP AMPLIFIER USING 3D SONNET BASED SVRM WITH PARTICLE SWARM OPTIMIZATION

AHMET KENAN KESKİN

IN PARTIAL FULFILLMENT OF THE REQUIREMENTS
FOR
THE DEGREE OF MASTER OF SCIENCE
IN

DEPARTMENT OF ELECTRONICS AND COMMUNICATIONS ENGINEERING

COMMUNICATIONS PROGRAM

ADVISOR
PROF. DR. FİLİZ GÜNEŞ

İSTANBUL, 2012

R.T.

YILDIZ TECHNICAL UNIVERSITY
GRADUATE SCHOOL OF NATURAL AND APPLIED SCIENCES

DESIGN OF AN ULTRAWIDE BAND MICROSTRIP AMPLIFIER USING 3D SONNET BASED SVRM WITH PARTICLE SWARM OPTIMIZATION

Thesis, which was prepared by Ahmet Kenan Keskin, has been adopted as MASTER THESIS at Yildiz Technical University Graduate School of Natural and Applied Science Department of Electronics and Communications on 28.06.2012 by following jury.

Advisor

Prof. Dr. Filiz GÜNEŞ

Yildiz Technical University

Members of The Jury

Prof. Dr. Filiz GÜNEŞ

Yildiz Technical University _____

Prof. Dr. Tayfun GÜNEL

Istanbul Technical University _____

Assist. Prof. Salih DEMİREL

Yildiz Technical University _____

PREFACE

This thesis has been prepared as Master Thesis in Yıldız Technical University Graduate School of Natural and Applied Science Department of Electronics and Communications Engineering Communications Program.

Nowadays, accurate and fast design systems require to compensate demands of rapidly developed micowave technology. In this thesis, fast and high accuracy model for microstrip lines is performed with support vector regression machine and then this model has been used to design an low noise ultra wide-band amplifier with particle swarm optimization.

I am very grateful to my mentor Prof. Dr. Filiz GÜNEŞ for completely supporting my thesis with her wisdom from beginning to ending. I also thanks to Assist. Prof. Salih Demirel and my research assistant friends for their helps. Finally, special thanks to my mother and aunts for their moral supports.

Haziran, 2012

Ahmet Kenan KESKİN

TABLE OF CONTENTS

Page

SYMBOL LIST

F_{req}	Required noise figure
F_{min}	Minimum noise figure
G_{Tmax}	Maximum transduce gain
G_{Treq}	Required transduce gain
VSWR	Voltage standing wave ratio
V_i	Input reflection
V_{ireq}	Required input reflection
ε	Insensitive loss function
ε_r	Relative dielectric permittivity of dielectric substrate
ε_{eff}	Effective relative dielectric permittivity of dielectric substrate
W	Width of microstrip conductor
T	Thickness of microstrip conductor
H	Heigth of dielectric substrate
f	Frequency
tanδ	Tangent loss
Z_0	Characteristic impedance

ABBREVIATION LIST

ANN	Artificial Neural Network
FDTS	Feasible Design Target Space
LNA	Low Noise Amplifier
SVRM	Support Vector Regression Machine
PSO	Particle Swarm Optimization
UWB	Ultra Wide Band

FIGURE LIST

TABLE LIST

ABSTRACT

DESIGN OF AN ULTRAWIDE BAND MICROSTRIP AMPLIFIER USING 3D SONNET BASED SVRM WITH PARTICLE SWARM OPTIMIZATION

Ahmet Kenan KESKİN

Department of Electronics and Communications Engineering

MSc. Thesis

Advisor: Prof. Dr. Filiz GÜNEŞ

In today's world, microwave technology has an important place for communication and military systems. With this growing importance, it is needed expeditious, high-accurate, feasible design systems. Therefore, 3D computer aided design has a significant role. Nowadays, 3D EM simulation programs are too thrived and it could give high-accurate results which are close to practical experiments. Although 3D simulations are so accurate; there is significant disadvantage like slowness. In order to solve this problem, one of the important methods is learning machines. Nonlinear learning machines are widely employed as the fast and flexible machines in the generalization of the highly nonlinear input-output discrete mapping relations in the microwave modeling. In this study, Support Vector Regression machine is used to model microstrip transmission line. Coarse and fine model of microstrip line is obtained. The SVRM model of microstrip line is high-accuracy like 3D EM simulation programs and fast like empirical formulations.

Microwave low noise amplifiers are used front-end element for receiver systems. Besides, an ultra wide-band(UWB) amplifier is useful for systems because of capability of multi-band operation. A robust and efficient design optimization of a microstrip amplifier is carried out so that geometry of all the microstrip lines W,L,T,ε_r,H,tanδ where W,L,T and ε_r,H,tanδ are the subvectors including widths, lengths and thicknesses of the microstrips and relative dielectric constant, height and loss of the selected substrate, respectively, can be obtained from the output to be used as the

input and output matching elements of a transistor subject to its potential performance. In the optimization procedure, the Electromagnetic (EM) - based Support Vector Regression Machine (SVRM) is employed to build the mapping relations between the characteristic impedance (Z_0)/the effective relative dielectric constant (ε_{eff}) of the equivalent transmission lines and the microstriplines W,L,T,ε_r,H as fast as a coarse model at the same time as accurate as a fine model. In the work, quasi-TEM microstripline synthesis formulas are used as a coarse database and the full-wave EM Simulator, Sonnet provides the fine Database. The source and load {$Z_S(\omega)$, $Z_L(\omega)$} termination couple corresponding to the compatible (Noise F(ω), Input VSWR $V_i(\omega)$, Gain $G_T(\omega)$,Bandwidth B) quadrates are utilized as the feasible design target resulted from the performance characterization of the selected high technology transistor subject to the Darlington theorem. Furthermore Particle swarm intelligence is successfully implemented as a comparatively simple and efficient algorithm in the optimization process of the input and output matching circuits. Finally typical design of a single transistor, microstrip, Ultra - Wideband (UWB) amplifier is presented as a worked example with the maximum gain, simultaneously ensuring the available minimum noise and a permitted small constant mismatching at each operation frequency, that corresponds to the ($F_{min}(\omega)$, V_{ireq}, $G_{Tmax}(\omega)$, B) quadrate.

Furthermore, performance of the resulted amplifier with the determined microstrip lines within the technological limitations is verified with Microwave Office AWRDE simulation program. Besides, the designed amplifier is fabricated and measured. Then, all of the results are compared each other.

Key words: Low noise, microwave amplifiers, particle swarm optimization, support vector regression machine, ultra wide band.

ÖZET

BİR ULTRA-GENİŞ BANDLI MİKROŞERİT KUVVETLENDİRİCİSİNİN 3-D SONNET TABANLI DVRM KULLANILARAK PARÇACIK SÜRÜ OPTİMİZASYONU İLE TASARIM

Ahmet Kenan KESKİN

Elektronik ve Haberleşme Mühendisliği Bölümü

Yüksek Lisans Tezi

Tez Danışmanı: Prof. Dr. Filiz GÜNEŞ

Günümüz dünyasında mikrodalga teknolojisi haberleşme sistemleri ve askeri sistemler için önemli bir yere sahiptir. Gittikçe artan önemiyle mikrodalga teknolojisi hızlı, yüksek doğruluklu tasarım sistemlerine ihtiyaç duymaktadır. Bu noktada 3 boyutlu bilgisayar destekli tasarım programları önemli bir rol oynamaktadır. Son zamanlarda pratik tasarıma yakın yüksek doğruluk sonuçlar verebilen 3 boyutlu elektromanyetik benzetim programları oldukça gelişti. Ancak, yüksek doğruluklu bu benzetim programlarının önemli bir dezavantajı yavaş olmalarıdır. Bu problemi çözmek için kullanılan önemli yöntemlerden biri öğrenen makinelerdir. Doğrusal olmayan öğrenen makineler mikrodalga modellemelerde doğrusal olmayan giriş ve çıkışlar için ayrık haritalama işlemlerinin genelleştirilmesinde kullanılan hızlı ve esnek makinelerdir. Bu çalışmada destek vector regresyon makineleri (DVRM) mikroşerit transmisyon hattının modellenmesi için kullanılmıştır. Bu kapsamda kaba ve hassas mikroşerit DVRM modelleri elde edilmiştir. Elde edilen mikroşerit DVRM modeli 3 boyutlu EM benzetim programları gibi yüksek doğruluklu ve analitik formülasyonlar gibi de hızlı çalışmaktadır.

Düşük gürültülü mikrodalga kuvvetlendiricileri alıcı sistemler için front-end elemanı olarak kullanılmaktadır. Ayrıca ultra-geniş bandlı kuvvetlendiriciler çoklu frekans bandlarında kullanıldıkları için birçok eleman yerine tek başına kullanılabilmektedirler. Bir mikroşerit kuvvetlendiricisinin tasarımı giriş çıkış uydurma devrelerinin mikroşerit

elemanlarının hat genişliği (W), uzunluğu (L), kalınlığı (T)ve kullanılan taban malzemesinin bağıl dielektrik katsayısı (ε_r), kalınlığı (H) gibi parametreleri ile kullanılan transistörün potansiyeline bağlı olarak optimizasyonla yapılabilir. Optimizasyon sürecinde mikroşerit hatların karakteristik empedans (Z_0) ve efektif bağıl dielektrik katsayısı (ε_{eff}) ile W,L,T,ε_r,H arasındaki bağlantı EM tabanlı DVRM kullanılarak sağlanmıştır. DVRM modeli elde edilirken kaba model eğitim verileri yarı-TEM mikroşerit sentez formülasyonlarından elde edilmiştir ve hassas model verileri SONNET EM benzetim programından sağlanmıştır. Hedeflenen gürültü F(ω), giriş yansıması $V_i(\omega)$, kazanç $G_T(\omega)$ ve band genişliği (B) değerlerine karşılık gelen kaynak ve yük uydurmaları $\{Z_S(\omega), Z_L(\omega)\}$ seçilen yüksek teknolojili bir transistörün Darlington teoremine bağlı olarak performans karakterizasyonu ile elde edilmiştir. Ayrıca giriş ve çıkış uydurma devrelerinin elde edilmesi için verimli ve basit bir algoritmaya sahip olan parçacık sürü optimizasyonu kullanılmıştır. Tasarım hedefleri maksimum kazanç, minimum gürültü ve düşük giriş yansıması olarak seçilen kuvvetlendiricinin giriş ve çıkış uydurmaları optimize edilip parametreleri elde edilmiştir.

Teknlojik sınırlamalar kapsamında elde edilen kuvvetlendirici Microwave Office AWRDE benzetim program kullanılarak doğruluğu kontrol edilmiştir. Ayrıca tasarlanan kuvvetlendirici üretilip ölçülmüştür. Son olarak, tüm sonuçlar karşılaştırmalı olarak incelenmiştir.

Anahtar Kelimeler: Destek vektör regresyon makinaları, düşük gürültü, kuvvetlendirici, parçacık sürü optimizasyonu, ultra-geniş band.

CHAPTER 1

INTRODUCTION

1.1 Literature Review

Computer-aided design (CAD) and electromagnetic (EM)- simulation-based design optimization become more and more important for the development of modern microwave devices and antennas since analytical models can only be used in the limited cases— for example for a limited operation bandwidth or initial designs that need to be further tuned to meet given performance specifications and required model accuracy. However, a serious bottleneck of EM simulation - driven optimizations are their high computational cost. It makes approaches employing EM solvers directly in the optimization loop very time-consuming or even impractical. This applies, in particular, to traditional gradient-based optimization involving numerous evaluations of the EM-simulation- based objective function. On the other hand, novel algorithms based on the multiagent search principle such as evolutionary algorithms, particle swarm optimizers are even more CPU-intensive although they permit to handle a number of issues, for example, lack of sensitivity information and presence of multiple local optima, which are problematic for the classical methods.

The model as fast as coarse models at the same time as accurate as fine models can be used for a computationally efficient CAD and EM-simulation-based optimization. Here, today's advances in the computational sciences provide great facilities to the electronics technology. Nonlinear learning machines which enable to generalize discrete data into the continuous data domain may be considered among these facilities. Nowadays, two typical nonlinear learning machines are widely employed as

the fast and flexible machines in the generalization of the highly nonlinear input–output discrete mapping relations in the microwave modeling: artificial neural-network (ANN) and support vector machine (SVM). A detailed literature for the utilization of the ANN techniques in the CAD of a variety of microwave components and circuits can be found in Zhang and Gupta [1].

On the other hand within the last decade, Vapnik's SVM theory [2] has been successfully applied in a wide range of classification and regression problems, based comprehensively on the powerful generalization capability of support vector machine (SVM) over other classical optimization techniques; especially its working principle based on the small sample statistical learning theory is utilized in lessening the need for the accurate training and validation data together with the human time.

1.2 Purpose of The Thesis

The purpose of this thesis is that an EM – simulation – based SVRM is generated to synthesize microstrip transmission lines as fast as coarse models and as accurate as fine models which will be used in this work as an optimization engine. After that, the obtained SVRM model will be used to design input and output matching circuit of an ultrawide band microstrip amplifier with PSO algorithm.

1.3 Hypothesis

Fast and high accurate SVRM model of microstrip transmission line could be obtained using 3D SONNET electromagnetic simulation program as data generator. The acquired model could be used to design input and output matching circuit of an ultrawide band microwave amplifier with high accuracy like 3D EM simulator but faster than EM simulator.

CHAPTER 2

MICROSTRIP TRANSMISSION LINES

Microstrip line is one of the most popular types of planar transmission lines, because of easy production and integration with active or passive microwave systems. Figure 2.1 shows geometry of a microstrip line. The thin conductor on the top side has width (W) and thickness (t), the bottom side is fully grounded, the dielectric substrate has thickness (h) and relative dielectric permittivity or constant (ε_r). It is presented that varied substrate materials which can be used to fabricate microstrip lines and their physical specifications in Figure 2.2.

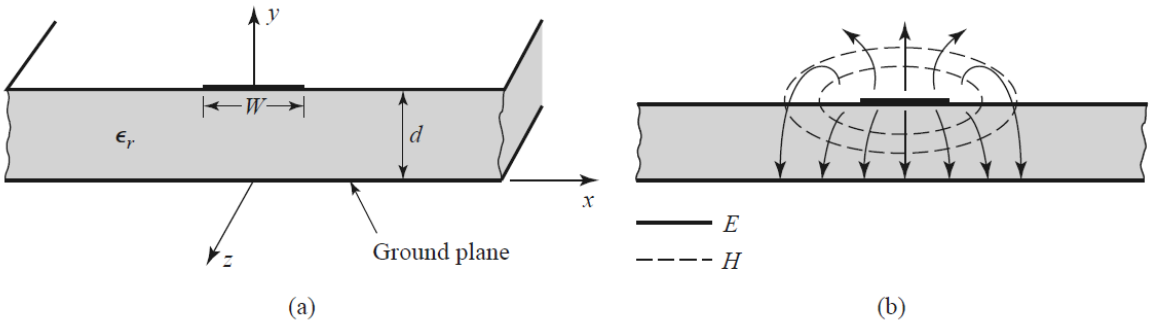

Figure 2. 1 Microstrip transmission line (a) Geometry (b) Electric and magnetic field lines

If there is no dielectric (ε_r=1), we could think the line as a two-wire line consisting of two flat strip conductors of width (W), separated by a distance 2h, because the ground could be removed via image theory. In this case, it could be said that the microstrip line has TEM mode propagation with phase velocity u_p = c and propagation constant k_0.

The presence of the dielectric, particularly the fact that the dielectric does not fill the region above the strip (y > d), complicates the behavior and analysis of microstrip line., Features of some dielectric substrates are given in Table 2.1. Unlike stripline, where all the fields are contained within a homogeneous dielectric region, microstrip has some (usually most) of its field lines in the dielectric region between the strip conductor and the ground plane and some fraction in the air region above the substrate. For this reason microstrip line cannot support a pure TEM wave since the phase velocity of TEM fields in the dielectric region would be c/ε_r , while the phase velocity of TEM fields in the air region would be c, so a phase-matching condition at the dielectric-air interface would be impossible to enforce.

Table 2. 1 Different PCB substrates and its specifications

Substrate	Relative Permittivity	Dielectric Strength (V/mil)	Loss Tangent
FR-4 Low Resin	4.9		0.008 @ 100 MHz
FR-4 High Resin	4.2		0.008 @ 3GHz
Alumina	9.6-10		0.0002 @ 1 GHz
Germanium	16		
Gallium Arsenide	13.1		0.0016 @ 10 GHz
Silicon	11.7-12.9	100-700	0.015 @ 10 GHz
Teflon	2.0-2.1	1000	0.00028 @3 GHz
Polyamide	2.5-2.6		
Polyethylene	2.26	450-1200	0.0031 @ 3GHz
RT/Duroid 5880	2.20		0.001 @ 1 GHz

In actuality, the exact fields of a microstrip line constitute a hybrid TM-TE wave and require more advanced analysis techniques than we are prepared to deal with here. In most practical applications, however, the dielectric substrate is electrically very thin ($d << \lambda$), and so the fields are quasi-TEM. In other words, the fields are essentially the same as those of the static (DC) case. Thus, good approximations for the phase velocity, propagation constant, and characteristic impedance can be obtained from static, or quasi-static, solutions. Then the phase velocity and propagation constant can be expressed as

$$v_p = \frac{c}{\sqrt{\varepsilon_{eff}}} \tag{2.1}$$

$$\beta = k_0\sqrt{\varepsilon_{eff}} \tag{2.2}$$

where ε_{eff} is the effective relative dielectric constant of the microstrip line. Because some of the field lines are in the dielectric region and some are in air, the effective relative dielectric constant satisfies the relation $1 < \varepsilon_{eff} < \varepsilon_r$ and depends on the substrate dielectric constant, the substrate thickness, the conductor width, and the frequency. The effective dielectric constant can be interpreted as the dielectric constant of a homogeneous medium that equivalently replaces the air and dielectric regions of the microstrip line, as shown in Figure 2.2. We will resent approximate design formulas for the effective dielectric constant, characteristic impedance, and attenuation of microstrip line; these results are curve-fit approximations to rigorous quasi-static solutions.

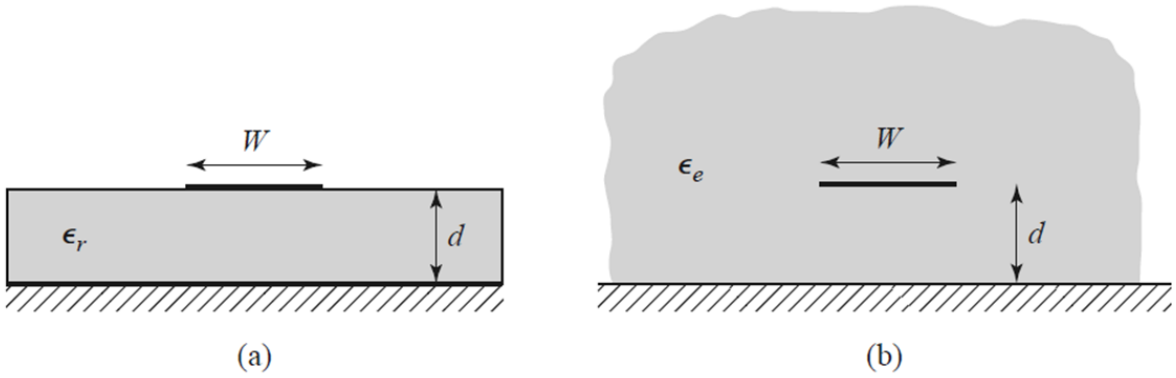

Figure 2. 2 Equivalent geometry of a quasi-TEM microstrip line (a) Original geometry (b) Equivalent geometry where the permittivity of substrate (εr) is replaced with a homogeneous medium of effective relative permittivity (εeff)

2.1 Formulations for Quasi-TEM Analysis of Microstrip Line

In practical applications, the empirical formulations, which give close results to full-wave analysis, could be used for calculations of microstrip line. These formulations are obtained by adding some numerical constants, which are acquired as a result of experimental studies, to analytical based formulations. The equations give us %99 accuracy compared with exact results.

The calculations of capacitance are given below formulas for a microstrip line which has W microstrip width, T thickness of strip, ε_r dielectric constant and H substrate thickness.

$$Ca = \frac{2\pi\varepsilon_o}{\ln\left(\frac{8H}{W}+\frac{W}{4H}\right)} \qquad , W/H \le 1 \tag{2.3}$$

$$= \varepsilon_o\left[\frac{W}{H}+1.393+0.667\ln\left(\frac{W}{H}+1.444\right)\right] \qquad , W/H > 1 \tag{2.4}$$

Strip line thickness is usually neglected. If the effect of strip line thickness (T) is calculated, W could be replaced with W_e.

$$We = W + 0.398T\left(1+\ln\frac{4\pi W}{T}\right) \qquad , W/H \le 1/2\pi \tag{2.5}$$

$$= W + 0.398T\left(1 + \ln\frac{2\pi}{T}\right) \qquad , W/H > 1/2\pi \tag{2.6}$$

After the calculation of microstrip line capacitance, the characteristic impedance (Z_c) of line can be found with Eq.2.8. Besides, effective relative dielectric constant (ε_{eff}) is given by Eq.2.7.

$$\varepsilon_{eff} = \frac{\varepsilon_r + 1}{2} + \frac{\varepsilon_r - 1}{2}\left(1 + \frac{12H}{W}\right)^{-\frac{1}{2}} + F(\varepsilon_r, H) - 0.217(\varepsilon_r - 1)\frac{T}{\sqrt{WH}} \tag{2.7}$$

$$Z_c = \frac{\sqrt{\varepsilon_{eff}}\sqrt{\mu_o\varepsilon_o}}{C} = \sqrt{\frac{\mu_o\varepsilon_o}{\varepsilon_{eff}}}\frac{1}{C_a} \tag{2.8}$$

Where;

$$F(\varepsilon_r, H) = 0.02(\varepsilon_r - 1)\left(1 - \frac{W}{H}\right)^2 \qquad , W/H \le 1 \tag{2.9}$$

$$0 \qquad , W/H > 1 \tag{2.10}$$

2.2 Microstrip Line Attenuation

Dielectric and conductor losses are caused atteunations. These losses are represented by series R for conductor loss and shunt G for dielectric loss in lumped-element equivalent circuit of a microstrip line. Atteunation constants are expressed as,

$$\alpha_c = \frac{R}{2Z_c} \tag{2.11}$$

$$\alpha_d = \frac{G}{2Y_c} \tag{2.12}$$

Total attenuation α is summation of those two equations. The attenuation is calculated as dB format with,

$$\alpha(dB) = 8,686\alpha \tag{2.13}$$

2.2.1 Dielectric Loss Attenuation

When the relative dielectric constant (ε_r) is complex, dielectric loss occurs. Tangent loss;

$$\tan\delta_l = \frac{\varepsilon''}{\varepsilon'} \approx \delta_l \tag{2.14}$$

$$\varepsilon = \varepsilon' - j\varepsilon'' \tag{2.15}$$

The connection between dielectric and tangent loss is given;

$$\alpha_d = \frac{GZc}{2} = \frac{\pi}{\lambda_o}\frac{\varepsilon_r}{\sqrt{\varepsilon_{eff}}}\frac{\varepsilon_{eff}-1}{\varepsilon_r-1}\tan\delta_l \tag{2.16}$$

There k_0=c/f. For example, for ε_r=9.7, ε_{eff}=9.7 and $\tan\delta_l$=2.10^{-4}, α_d is $1{,}52.10^{-3}$ Np/m. The dielectric loss is very small compared to conductor loss.

2.2.2 Conductor Loss

Conductor of a microstrip line has loss because it is not perfect electric conductor. Because of this loss, transmitted energy on the line is converted to thermal energy. Conductor loss of microstrip is represented with series resistor (R_1). Attenuation due to conductor loss is formulated as follows,

$$\frac{R_1 W}{R_m} = LR\left(\frac{1}{\pi} + \frac{1}{\pi^2}\ln\frac{4\pi W}{T}\right) \tag{2.17}$$

Where LR is loss rate and R_m is skin depth effect. Those are expressed as;

$$LR = 1 \qquad , \frac{W}{H} \le 0.5 \tag{2.18}$$

$$LR = 0.94 + 0.132\frac{W}{H} - 0.0062\left(\frac{W}{H}\right)^2 \qquad , \; 0.5 < \frac{W}{H} \le 10 \tag{2.19}$$

$$R_m = (\omega\mu/\sigma)^{\frac{1}{2}} \tag{2.20}$$

R_2 is resistor of the ground plane.

$$W\frac{R_2}{R_m}=\frac{W/H}{W/H+5.8+0.03\ W/H} \qquad ,0.1\le\frac{W}{H}\le 10 \tag{2.21}$$

Total resistor can be represented with R_1+R_2.

$$\alpha_c=\frac{R_1+R_2}{2Z_c} \tag{2.22}$$

Total attenuation;

$$\alpha=\alpha_d+\alpha_c \tag{2.23}$$

In there, dielectric loss (α_d) is very smaller than conductor loss (α_c). Thus, α_d can be neglected.

2.3 Higher Frequency Behavior of Microstrip Line

Quasi-TEM equations of microstrip line could be accepted as sufficiently accurate from 2 GHz to 4 GHz for a substrate which has 1 mm dielectric thickness. If the dielectric thickness of the substrate is 0,5 mm, frequency limit will be 4-8 GHz for accuracy. If these frequency limitations are exceeded, it should take into account that dispersion of effective dielectric constant and variation of characteristic impedance depends on frequency. In higher frequencies, the electric field concentrates between strip line and ground plane therefore effective dielectric constant and attenuation increases. Furthermore, conductor loss increases because most of the current will flow at the inner face of microstip and resistivity of skin depth (R_m).

The formulations microstrip lines for higher frequency are given below;

$$\varepsilon_{eff}(f)=\varepsilon_r-\frac{\varepsilon_r-\varepsilon_{eff}(0)}{1+\left(\frac{f}{f_a}\right)^m} \tag{2.24}$$

$$Z_o(f)=Z_o\left(\frac{\varepsilon_{eff}(0)}{\varepsilon_{eff}(f)}\right)^{\frac{1}{2}}\frac{\varepsilon_{eff}(f)-1}{\varepsilon_{eff}(0)-1} \tag{2.25}$$

where,

$$f_a = \frac{f_b}{0.75 + (0.75 - 0.332\varepsilon_r^{-1.73})W/H} \tag{2.26}$$

$$f_b = \frac{47.746}{H\sqrt{\varepsilon_r - \varepsilon_{eff}(0)}} \tan^{-1} \varepsilon_r \sqrt{\frac{\varepsilon_{eff}(0) - 1}{\varepsilon_r - \varepsilon_{eff}(0)}} \tag{2.27}$$

$$m = m_o m_c \leq 2.32 \tag{2.28}$$

$$m_o = 1 + \frac{1}{1 + \sqrt{W/H}} + 0.32(1 + \sqrt{W/H})^{-3} \tag{2.29}$$

$$m_c = 1 + \frac{1.4}{1 + W/H}(0.15 - 0.235e^{-0.45 f/f_a}) \qquad W/H \leq 0.7 \tag{2.30}$$

$$= 1 \qquad W/H > 0.7 \tag{2.31}$$

CHAPTER 3

SUPPORT VECTOR REGRESSION MACHINES

Nowadays, two typical nonlinear learning machines are widely employed as the fast and flexible machines in the generalization of the highly nonlinear input-output discrete mapping relations in the microwave modeling: Artificial Neural-Network (ANN) and Support Vector Machine (SVM). A detailed literature for the utilization of the ANN techniques in the CAD of a variety of microwave components and circuits can be found in Zhang and Gupta [1]. On the other hand within the last decade, Vapnik's SVM theory [2] has been successfully applied in a wide range of classification and regression problems, resulting in its improved generalization performance over other classical optimization techniques. This is mainly because, firstly, SVM solves a convex constrained quadratic optimization problem, whose error surface is free of local minima and has a unique global optimum; secondly, SVM approach is based on structural risk minimization (SRM) principle instead of empirical risk minimization (ERM) which is used in ANN approach. SRM principle implements well trade-off between the model's complexity and its generalization ability [3]. Furthermore, SVM is based on small sample statistical learning theory, whose optimum solution is based on limited samples instead of infinite sample that ensures enormous computational advantages.

3.1 SVRM Theory

Given a training dataset $(x_i, y_i), i = 1, 2, ..., \ell$ where $x_i \in R^n, y_i \in R$ and ℓ is the size of training data, SVR tries to find the mapping function $f(x)$ between the input variable vector x and the desired output variable y. In formula this read as:

$$f(x) = w^T \cdot \phi(x) + b \tag{3.1}$$

where $x^T = (x_1, ..., x_n) \Rightarrow \phi^T(x) = (\phi_1(x), ..., \phi_N(x))$ and $b \in R$.

This step is equivalent to mapping the input space x into a new space, $F = \{\phi(x) / x \in X^n\}$. Thus, $f(x)$ is a nonlinear function in the x-input space and linear function in the F-feature space. Thus, we will build a nonlinear machine in two steps: First, a fixed nonlinear mapping vector $\varphi(x)$ transforms the data into a feature space F, and then the linear machine built in this feature space is used to perform regression on the data. In this manner, we will refer to quantities w and b in (3.1) as the weight vector and bias where w is:

$$w^T = (w_1, w_2, ..., w_N) \tag{3.2}$$

Traditional regression method finds the regression function $f(x)$ by determination of w and b using the rule of empirical risk minimization principle:

$$R_{emp}[f] = \frac{1}{l}\sum_{i=1}^{\ell} L(x_i, y_i, f) \tag{3.3}$$

Where $L(x_i, y_i, f)$ represent an error (loss) function. One of the familiar loss functions is ε-insensitive loss function developed by Vapnik [4]:

$$L(f(x_i) - y_i) = |y - f(x)|_{\varepsilon} = \max|0, |y - f(x)| - \varepsilon| \tag{3.4}$$

However, the actual risk minimization cannot be realized only with the empirical risk minimization [2]. A typical example is the over-fitting of ANN. By the SRM principle employes by the SVR, the generalization accuracy is optimized over the empirical error and the flatness of the regression function which is guaranteed on a small w:

$$R_{SRM}(f, w) = \frac{1}{2}\|w\|^2 + CR_{emp}[f] \tag{3.5}$$

where $\frac{1}{2}\|w\|^2$ is the term characterizing the modeling complexity and C is a regularization parameter which determines the trade-off between model complexity and empirical loss function. Substituting (3.3),(3.4) into (3.5) and introducing the slack

variables ξ_i, ξ_i^*, Eq. (3.5) is transformed into the following soft margin primal optimization problem:

Minimize:

$$\frac{1}{2}\|w\|^2 - C\sum_{i=1}^{\ell}\left(\xi_i + \xi_i^*\right) \tag{3.6}$$

subject to:

$$\left(\left\langle w \cdot \phi(x_i)\right\rangle + b\right) - y_i \le \varepsilon + \xi_i \tag{3.7}$$

$$y_i - \left(\left\langle w \cdot \phi(x_i)\right\rangle + b\right) \le \varepsilon + \xi_i^* \tag{3.8}$$

$$\xi_i \ge 0, \xi_i^* \ge 0, \varepsilon \ge 0, i = 1, 2, ..., \ell \tag{3.9}$$

Combining the objective function given in (3.6) with constraints in (3.7-3.9), we have the corresponding Lagrangian function. By applying saddle point conditions with respect to the primal variables w_i, b, ξ_i, ξ_i^* leads to the optimal regressor (i.e., optimal set of the weighting values), given by

$$w = \sum_{i=1}^{\ell}\left(\alpha_i^* - \alpha_i\right)\phi(x_i) \tag{3.10}$$

where α_i, α_i^* are positive Lagrangian multipliers obtained by maximization of the following dual space objective function:

$$W(\alpha, \alpha^*) = -\varepsilon\sum_{i=1}^{\ell}\left(\alpha_i^* + \alpha_i\right) + \sum_{i=1}^{\ell} y_i\left(\alpha_i - \alpha_i^*\right) - \frac{1}{2}\sum_{i,j=1}^{\ell}\left(\alpha_i^* - \alpha_i\right)\left(\alpha_j - \alpha_j^*\right)\left\langle \phi(x_i)\phi\left(x_j\right)\right\rangle \tag{3.11}$$

subject to:

$$0 \le \alpha_i \le C, 0 \le \alpha_i^* \le C, i = 1, ..., n, \sum_{i=1}^{\ell}\alpha_i = \sum_{i=1}^{\ell}\alpha_i^* \tag{3.12}$$

The corresponding Karush-Kuhn-Tucker complementary conditions are:

$$\alpha_i\left(\left\langle w \cdot \phi(x_i)\right\rangle + b - y_i - \varepsilon - \xi_i\right) = 0 \tag{3.13}$$

$$\alpha_i^*\left(y_i - \left\langle w \cdot \phi(x_i)\right\rangle + b - \varepsilon - \xi_i^*\right) = 0 \tag{3.14}$$

$$\xi_i \cdot \xi_i^* = 0 \tag{3.15}$$

$$\alpha_i \cdot \alpha_i^* = 0 \tag{3.16}$$

$$(\alpha_i - C) \cdot \xi_i = 0 \tag{3.17}$$

$$(\alpha_i^* - C) \cdot \xi_i^* = 0, i = 1, 2, ..., \ell \tag{3.18}$$

From (3.13) and (3.14) of the Karush-Kuhn-Tucker conditions, it follows that for only the samples satisfying $|f(x_i) - y_i| \geq \varepsilon$, the Lagrangian multipliers may be nonzero, and for the samples of $|f(x_i) - y_i| < \varepsilon$, the Lagrangian multipliers α_i, α_i^* vanish. Since the products of α_i with α_i^* and ξ_i with ξ_i^* according to (3.15) and (3.16) are zero, at least one term in the couples of (α_i, α_i^*); (ξ_i, ξ_i^*) is zero. Therefore we have a sparse expansion of w in terms of input variable vector x; thus we do not need all data to describe w. The samples (x_i, y_i) that come with nonvanishing coefficients are called Support Vectors (SVs). The idea of representing the solution by means of a small subset of training points has also enormous computational advantages. This reduced number of nonzero parameters together with the guaranteed global minimum gains superiority to SVM over alternative methods. A detailed mathematical background together with literature can be found in Vapnik [2].

Thus, substituting the calculated nonzero Lagrangian multiplier $(\alpha_i s)$ into (3.10) and then into (3.1), the mapping function $f(x)$ between the input variable space and the desired output variable can be expressed in terms of the SVs as follows:

$$f(x) = \sum_{i=1}^{ns} \alpha_i y_i \left\langle \phi(x_i) \phi(x_j) \right\rangle + b \tag{3.19}$$

Where b can be found making use of the primal constraints in (3.13), (3.14) and ns is the number of the SVs. The inner product $\left\langle \phi(x_i) \phi(x) \right\rangle$ in the feature space is called Kernel function K, which can be given for all x, z, X as:

$$K(x, z) = \left\langle \phi(x) \phi(z) \right\rangle \tag{3.20}$$

where ϕ is a mapping from X to an inner product feature space F. Substituting (3.21) into (3.20), we have the SV expansion of $f(x)$ in the terms of kernels as:

$$f(x) = \sum_{i=1}^{ns} \alpha_i y_i K(x_i, x) + b \tag{3.21}$$

For more detailed information about SVRM theory, it could be looked to Cristianini and Shawe-Taylor [5].

CHAPTER 4

3-D SIMULATION BASED MICROSTRIP MODELING WITH SVRM

ANN and SVRM are once trained, they are capable of responding almost instantly to any input variable set, and thus they are as fast as the approximate (coarse) models and can be as accurate as the detailed electromagnetic (fine) models. Here, the key problem is to train these machines with the accurate data which may be measured or simulated data. In modeling using these nonlinear learning machines, accurate training data generation is the major constituent of the total model development time as it needs both CPU and human time. Recently, there is a new trend in the Electromagnetic (EM)-ANN area for searching the techniques using reduced number of accurate training data, thus resulting in lessened CPU and human time together with faster model development. The pioneering techniques for reducing the need for accurate training data can be given as follows: Neural networks with knowledge such as the knowledge-based neural networks (KBNN) , difference method (DM) [6], prior-knowledge input (PKI) [7] network and space mapped neural networks (SMNN) [8],[9],[10],[11]. Furthermore an efficient knowledge-based automatic model generation (KAMG) [12],[13] technique is proposed combining automatic model generation, knowledge neural networks, and space mapping, where the two data generators —coarse and fine generators— are simultaneously employed for the first time.

In design of microwave circuits which include microstrip line, 3 dimension electromagnetic (3-D EM) simulation program should be used for higher accuracy because these simulation programs analyze the microstrip line as full-wave. However,

there are some disadvantages of 3-D EM simulations like slowness and higher computer hardware requirements.

In this thesis, it is proposed to overcome those problems with microstrip modeling using 3-D EM simulation based SVRM. In order to realize the modelling there are two important stages: coarse model and fine model. First of all, SVRM is trained with empirical formulations of microstrip data in coarse model. Then, the support vectors (SVs) taking from coarse model is trained with 3-D EM simulation data of microstrip. These second stages either increase the accuracy because of simulations or decrease required data number because of SVs. The draft of model is shown in Figure 4.1.

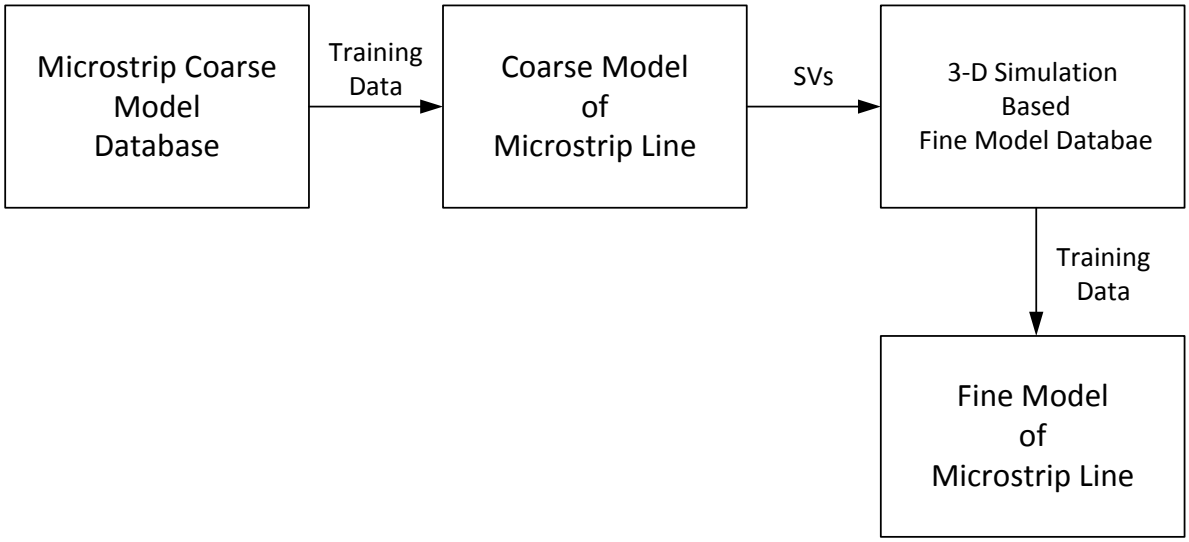

Figure 4. 1 SVRM modelling of microstrip Line

4.1 Coarse Model of Microstrip Line

In coarse model of microstrip line, SVRM is trained with data which is obtained by empirical formulations. Width (W) of microstrip line, height (H) and dielectric permittivity (ε_r) of substrate, frequency (f) are defined as input data. Characteristic impedance (Z_0) of the line and effective dielectric constant (ε_{eff}) is used as output data. The model is presented in Figure 4.2. 1000 data sets are used for training. Data sets are taken some of intervals. The range of values for input and output is described as Table 4.1.

Table 4. 1 The range of values for SVRM training dataset

	Start Value	Stop Value	Increment interval
Width (W)	0.1 mm	4.6 mm	0.5 mm
Height (H)	0.1 mm	2.2 mm	0.7 mm
Permittivity (ε_r)	2	10	2
Frequency(f)	2 GHz	14 GHz	3 GHz
Characteristic Impedance (Z_0)	3 ohm	240 ohm	
Effective Permittivity (ε_{eff})	1.5	9.7	

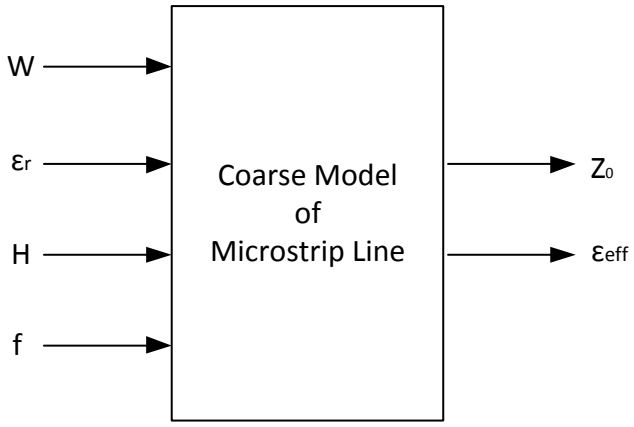

Figure 4. 2 Coarse model input output

Each learning machine generates only an output. Therefore, there are two machines for two outputs. Besides, epsilon-SVR is used for training and radial basis function is taken as kernel. After the training, SVRM model interpolates the value except training data. Furthermore, SVRM gives us support vectors, these vectors are used to constitute the fine model. The training results of the model are presented in Fig 4.3, 4.4, 4.5.

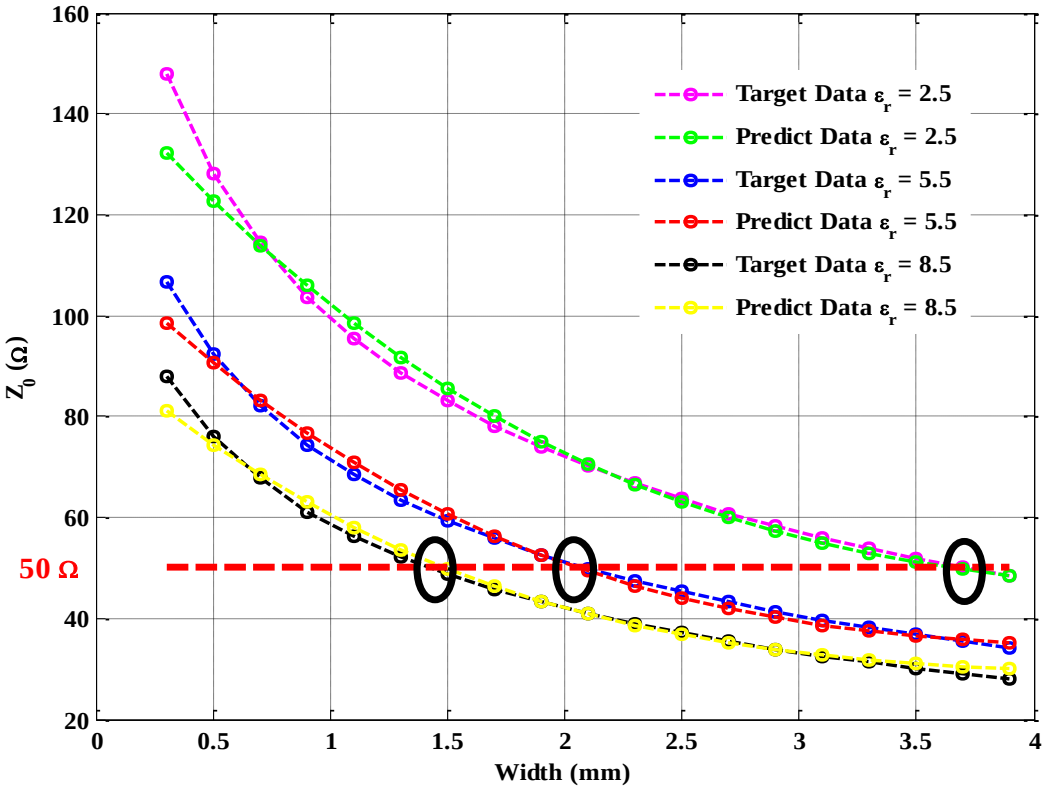

Figure 4. 3 Characteristic impedance vs. width for coarse model

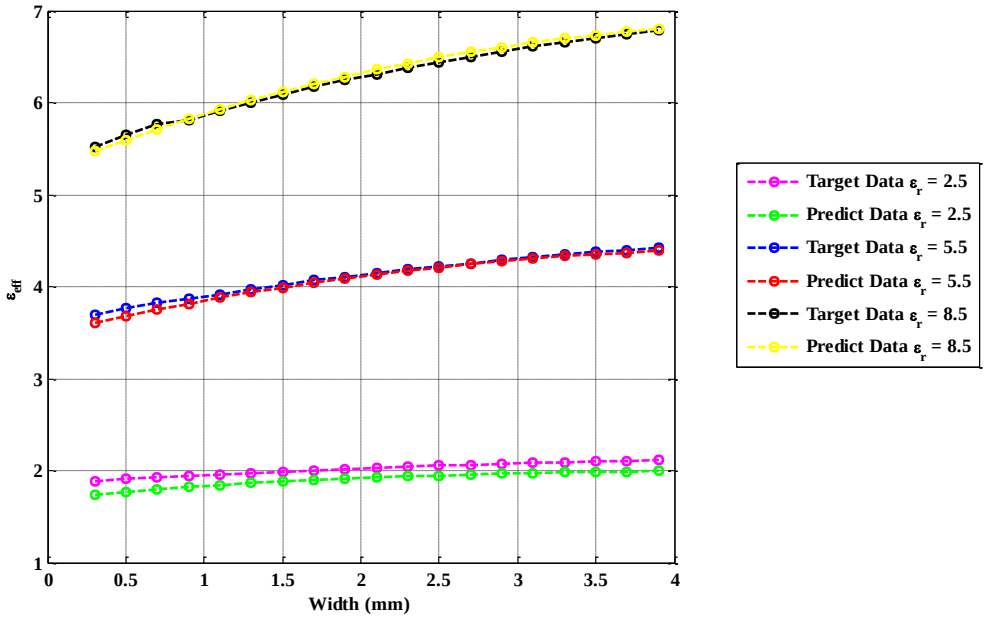

Figure 4. 4 Effective relative dielectric constant vs. width for coarse model

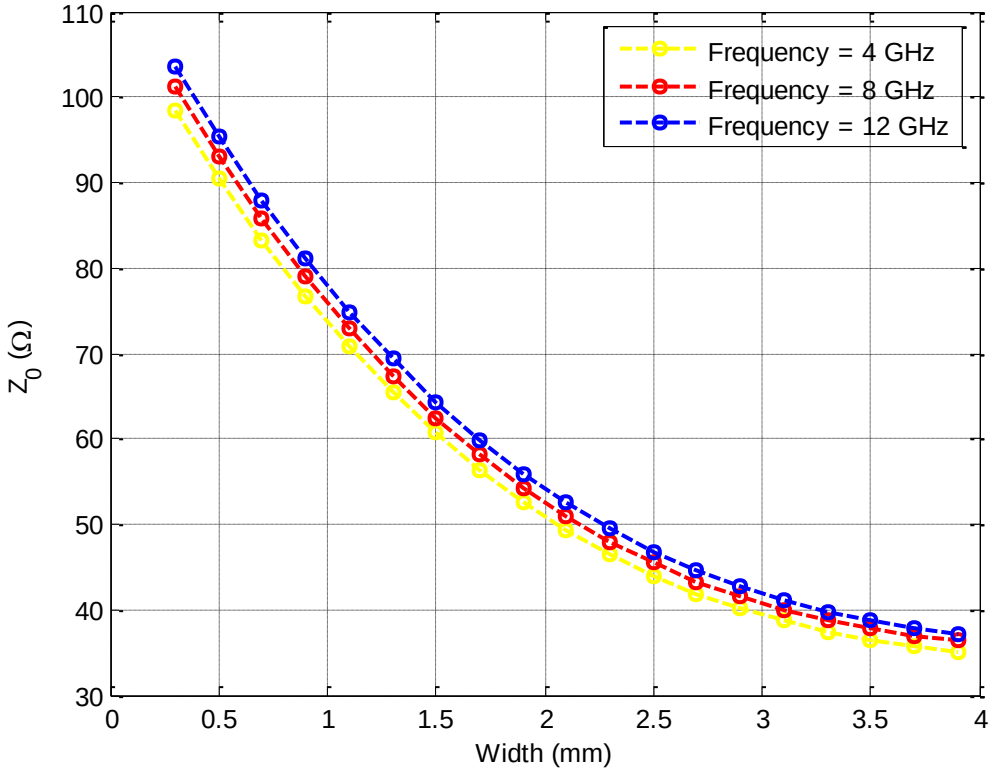

Figure 4. 5 Characteristic impedance depends on frequency for coarse model

Accuracy of coarse model is given in Table 4.2. In the table, the accuracy of characteristic impedance results and SVs number of model is compared for different ε values. It is chosen for fine model second ε value. The accuracy formulation is given as;

$$\%error = (1 - \frac{\sum \left| x_{predict} - x_{target} \right|}{\sum x_{target}}) x100 \quad (4.1)$$

Table 4. 2 Accuracy and SVs number depends on ε

Epsilon	Accuracy	Number of SVs
0.05	%99.4	583
0.07	%98.6	402
0.1	%97.9	279

4.2 Fine Model of Microstrip Line

In order to build fine model of microstrip line, support vectors (SVs) taking from the coarse model are used. Training data set is formed with reference to SVs, namely input values of training data, which are W, H, ε_r, f are same with inputs of SVs. Output values of training data, which are Z_0 and ε_{eff}, are obtained by SONNET 3-D simulation program. SONNET 3-D simulation program uses method of moments to solve EM problems and analyzes the structures as fullwave [14]. Therefore, training data set is exact solution; it means higher accuracy for model. Besides, the training data set number is less than coarse model because SVs number is training data set number. Consequently, fine model is a very fast model comparing with 3-D simulation program. The fine model is represented in Figure 4.6.

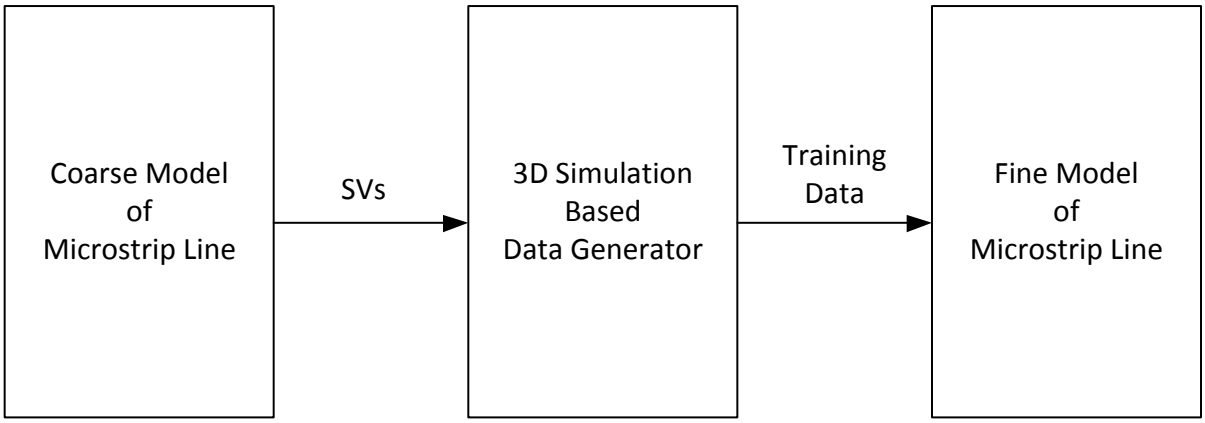

Figure 4. 6 Fine model of microstrip Line

The SVs numbers, which are acquired from coarse model, are 402 for Z_0 and 367 for ε_{eff} , this is also training data set number of fine model. Kernel function and SVR type are same with coarse model. Following figures give us the results of fine model. In fine model, ε value of SVRM is taken as 0.01 and the accuracy of results is %99.4. The compared results for fine model are presented in Fig 4.7, 4.8, 4.9.

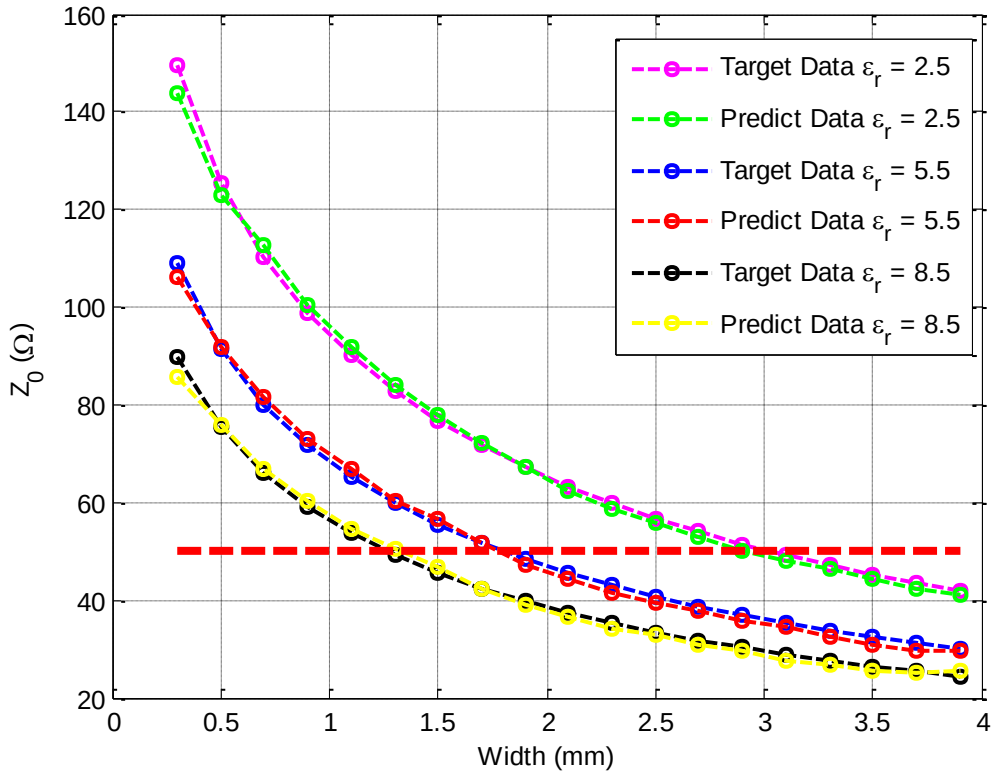

Figure 4. 7 Characteristic impedance vs. width for fine model

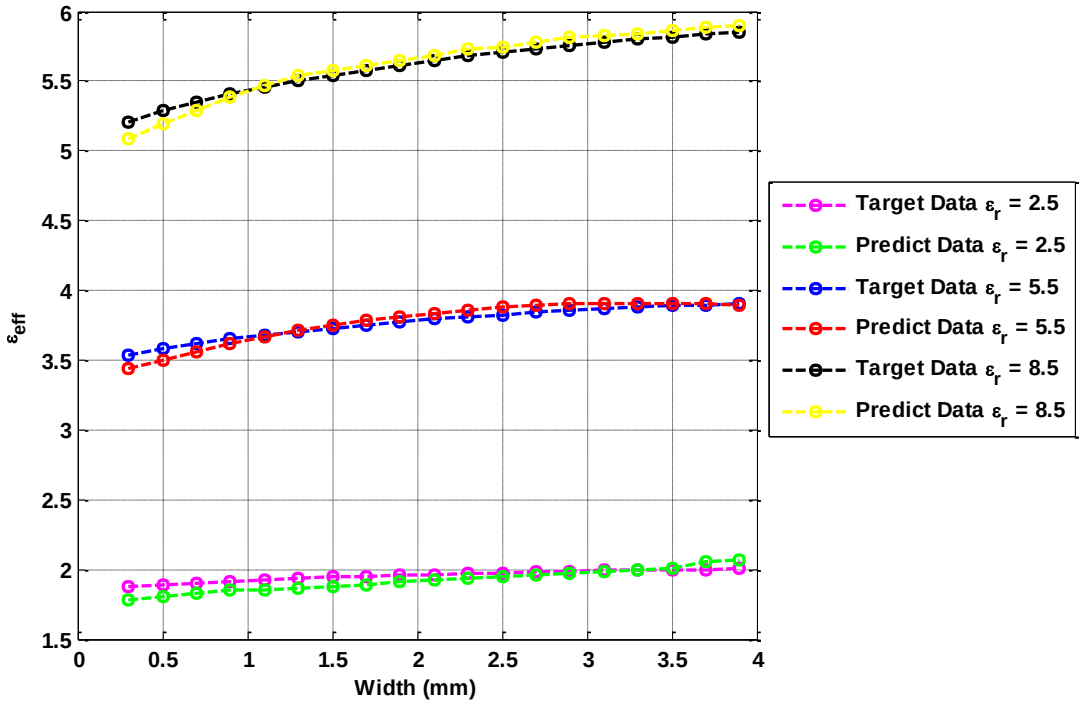

Figure 4. 8 Effective relative dielectric constant vs. width for fine model

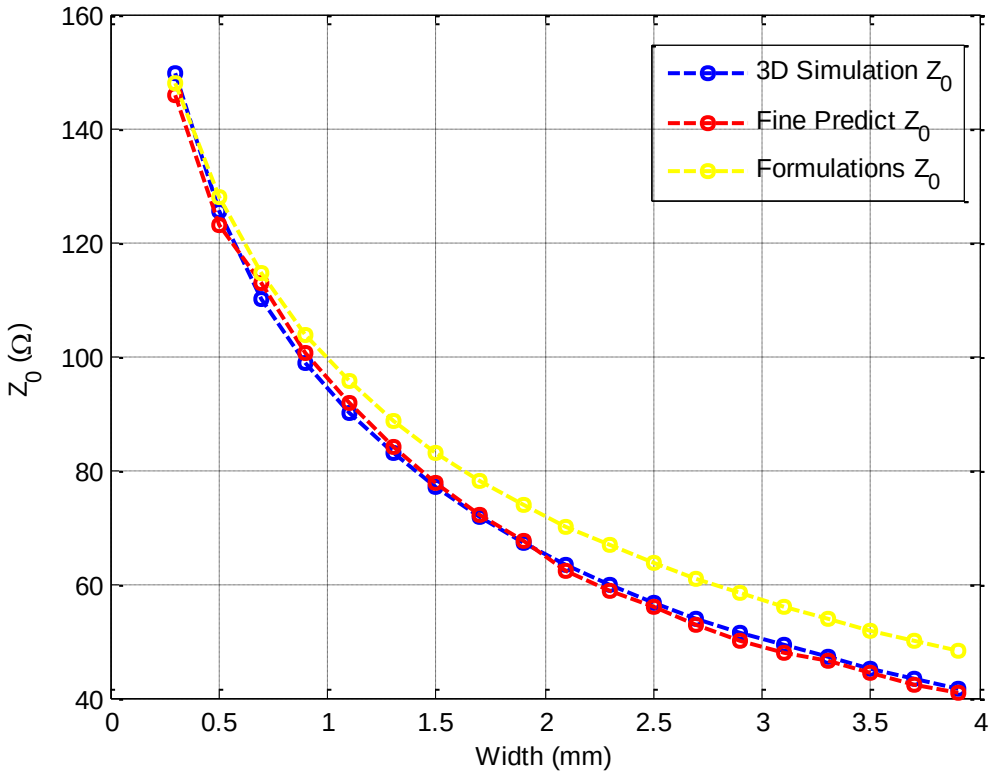

Figure 4. 9 Comparative characteristic impedance results for fine predict, 3D simulation and empirical formulation data

4.3 Conclusion

In this section, the high-accuracy and fast SVRM model of a microstrip line is built up. First of all, coarse model is constructed with empirical formulation data. In order to do this, epsilon-SVR type is used. Accuracy of results and SVs number according to epsilon value of the SVRM is given in Table 4.2. Afterward, the fine model is built using SVs from coarse model. Fine model results are too close to exact solution of microstrip line because the database of fine model is acquired by 3D EM simulation data. Besides, there is important difference between 3D EM simulation and SVRM model; the SVRM model is faster than simulation. Elapsed time for SVRM prediction is 0.005 seconds and elapsed time for SONNET solver is 2 seconds. Elapsed time data is computed at a computer has 2.1 GHz CPU and 3 GB RAM. It means that SVRM model is 400 times faster than SONNET solver. This pace of SVRM is very important for multiple calculations.

CHAPTER 5

PERFORMANCE CHARACTERIZATION AND AMPLIFIER DESIGN

5.1 Performance Characterization

It is important that the rigorous analysis of performance capabilities for the chosen transistor to obtain the Feasible Design Target Space (FDTS) to design an amplifier. Otherwise is to utilize the device either under its potential performance or for unrealizable requirements. FDTS for a low-noise amplifier can be defined as determination of the compatible (Noise figure F, Input VSWR Vi, Gain GT) triplets and their source Z_S and load Z_L terminations at the chosen operation conditions of the device. Modeling the small signal amplification behavior of the transistor as a linear two-port, this device characterization problem is solved point by point in the operation domain of the device in [15],[16] two main stages as follows: First, all the performance measure functions which are stability, transducer gain GT, input VSWR Vi, and noise figure F are represented altogether at the input impedance Zin—plane as a design configuration so that one can easily observe design tradeoff relations together with all the resulting compatible/incompatible (F, Vi, GT) triplets at the chosen operation conditions of the device; triplet example is given in Figure 5.1. In the final stage, an analytical formulation of the maximum gain GTmax constrained by the" required noise Freq and input VSWR Vireq and the corresponding source Z_{Smax} and load Z_{Lmax} are obtained on the rigorous geometrical bases within the physical limitations of the employed device.

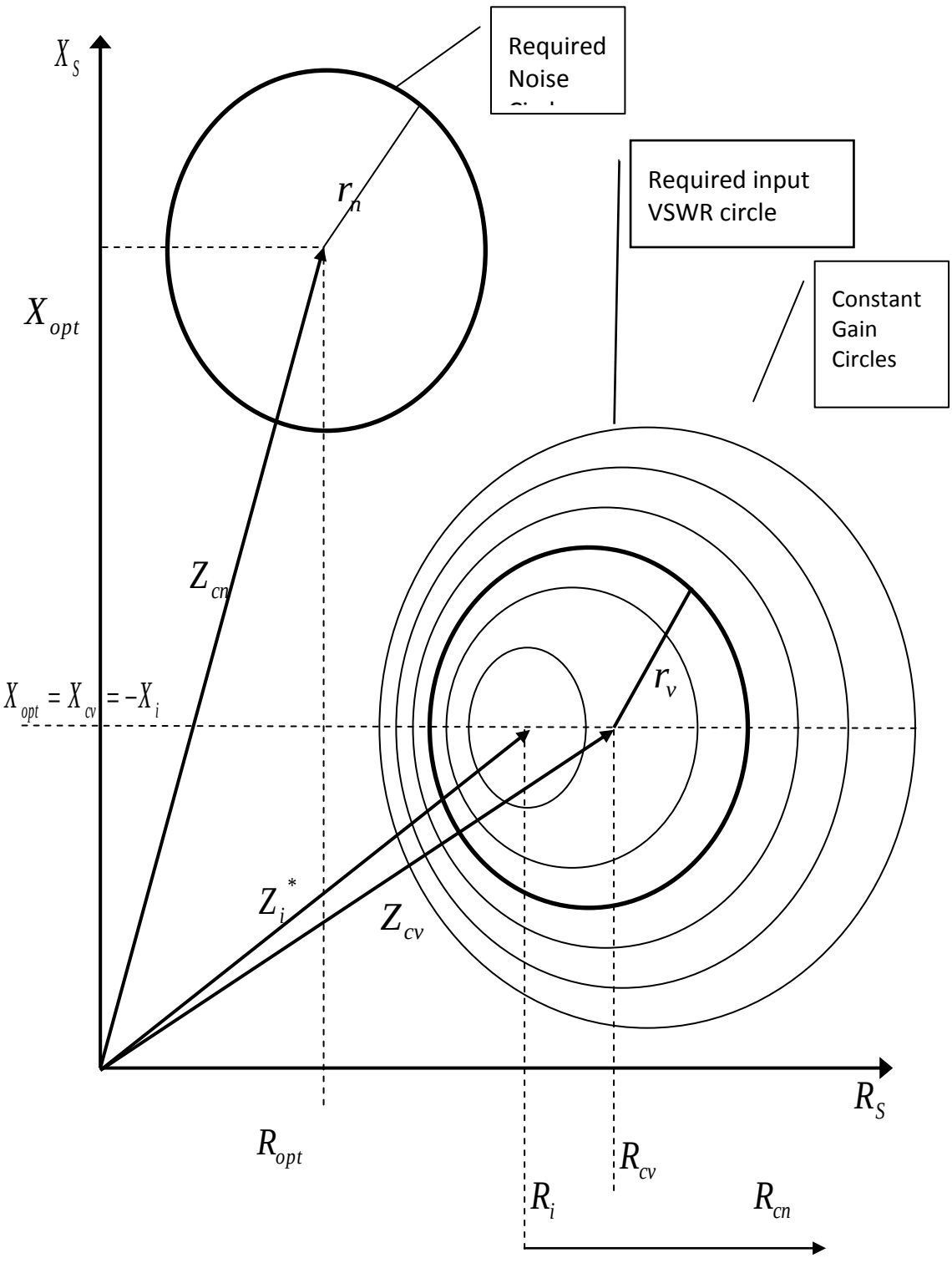

Figure 5. 1 VSWR, gain and noise triplets at Zin plane

Then, combining this performance characterization with the Artificial Neural Networks (ANN) or/Support Vector Regression Machine (SVRM) model of the device [4],[17] the compatible (Noise Figure F, Input VSWR Vi, Gain GT) triplets together with their source ZS and load ZL terminations can be obtained as the functions of the operation variables VDS, IDS, f of the device; thus this approach can result in the whole performance data sheets for the device [18]. It should be noted here that performance characterization of an active device is an interdisciplinary field and hence requires sufficient knowledge of all related disciplines such as linear circuit theory, noise theory, microwave theory, and CAD tools. However, nowadays derivative-free, evolutionary global optimum searchers such as genetics, simulated annealing, ant colony, and particle swarm optimization are developed and commonly employed in a wide-range of electromagnetic engineering problems, particularly nowadays, particle swarm optimization is very popular since its implementation is simpler, faster, and more efficient than the others. In this work, we formulate the feasible target space at a chosen operation condition as a constrained optimization problem and we utilize the particle swarm intelligence as a global optimum searcher in the optimization process and then compare the results with the ones of the performance characterization theory. Thus, we present a simple and efficient approach to be used during the design process of a low-noise amplifier, to determine the feasible design target at a chosen operation point of the device without having need for more complicated knowledge and soft-ware.

5.2 Amplifier Design

In a typical design problem of a basic microwave amplifier employing per se a FET as an active device, the active device can be represented by a linear two-port [Figure 5.2(a)] specified by its compatible (F, Vi, GT) performance triplets and their (ZS, ZL) terminations at each point within its operation domain. Furthermore, the ZS and ZL terminations can also be modeled by their Darlington equivalencies by means of the front- and back-end matching networks [Figure 5.2(b)], respectively. Here, the passive (ZS, ZL) termination pair is the simultaneous solutions of the following nonlinear

performance F, Vi, GT equations of the transistor subject to the physical realization conditions [16]:

$$F \triangleq \frac{(S/N)_i}{(S/N)_o} = F\{Z_S\} = F_{\min} + \frac{R_n}{|Z_{opt}|^2}\frac{|Z_s - Z_{opt}|^2}{R_s} \tag{5.1}$$

$$V_i = V_i\{R_s, X_s, R_L, X_L\} = \frac{1+|\rho_{in}|^2}{1-|\rho_{in}|^2}, |\rho_{in}| = \left|\frac{Z_S - Z_{in}^*}{Z_S + Z_{in}}\right| \tag{5.2}$$

$$G_T\{Z_S, Z_L\} = \frac{P_L}{P_{AVS}} = \frac{4.R_S.R_L|z_{21}|^2}{|(z_{11}+Z_S)(z_{22}+Z_L) - z_{12}.z_{21}|^2} \tag{5.3}$$

Here, the physical realization conditions can be expressed as

follows:

$$\mathrm{Re}\{Z_{in}\} = \mathrm{Re}\left\{z_{11} - \frac{z_{12}z_{21}}{z_{22}+Z_L}\right\} > 0 \tag{5.4}$$

$$\mathrm{Re}\{Z_{out}\} = \mathrm{Re}\left\{z_{22} - \frac{z_{12}z_{21}}{z_{11}+Z_S}\right\} > 0 \tag{5.5}$$

$$F_{req} > F_{\min}, V_{ireq} > 1, G_{T\min} \le G_T \le G_{T\max} \tag{5.6}$$

Where, $z_{ij} = r_{ij} + jx_{ij}; i, j = 1, 2$ are open-circuited parameters, whereas $F_{\min}, R_N, Z_{opt} = R_{opt} + jX_{opt}$ are the noise parameters of the transistor at the chosen operation conditions, and the conditions given by Eqs. (5.4) and (5.5) ensures the stable operation of the active device. Here, to determine the design target space for a low-noise amplifier, the problem can be considered into two parts as follows: In the first part, upper limitation of the gain $G_{T\max}$ should be determined with its passive $Z_{S\max}, Z_{L\max}$ termination pair.

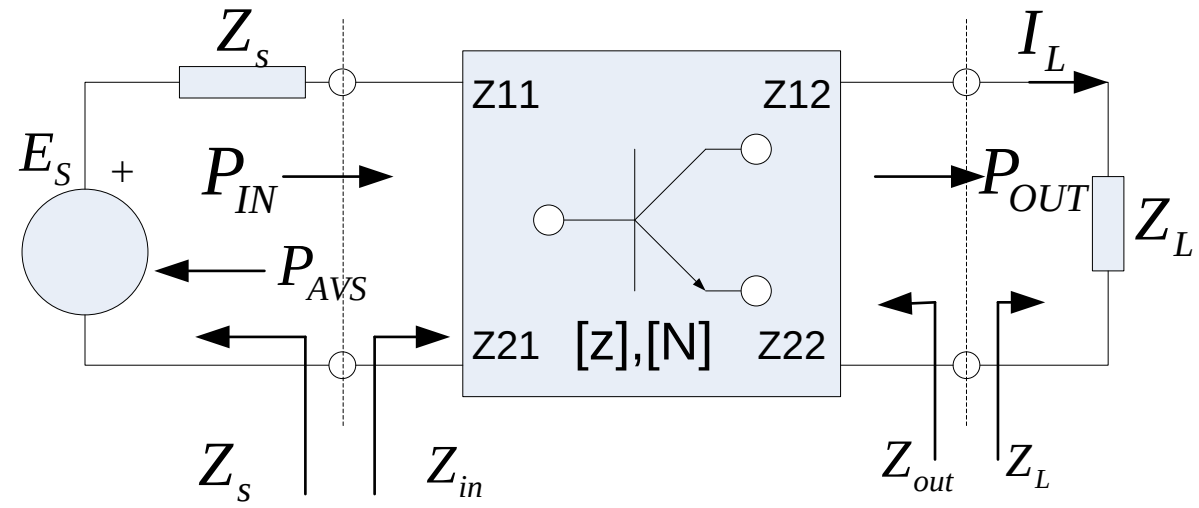

(a)

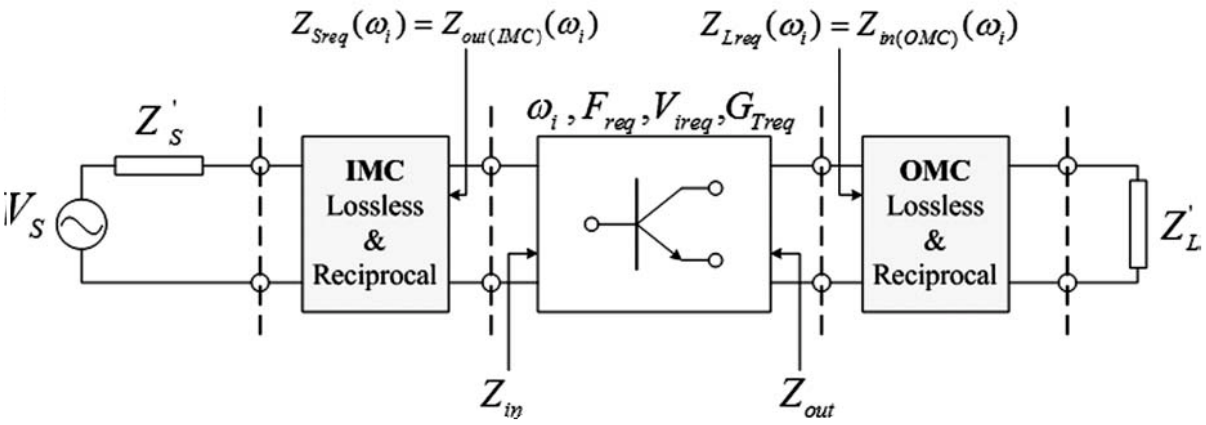

(b)

Figure 5. 2 (a) Transistor with the compatible performance terminations (b) Transistor with the Darlington equivalencies for the ZS(w), ZL(w) terminations.

This problem can be described as a mathematically constrained maximization to find out the maximum value of $G_T(R_S, X_S, R_L, X_L)$ given by Eq. (5.3) for the passive ZS and ZL terminations satisfying the stability conditions given by Eqs. (5.4) and (5.5) subject to the constraints of the following:

$$\Phi_1 = F_{req} - F(R_S, X_S) \text{ and } \Phi_2 = V_{ireq} - V_i(R_S, X_S, R_L, X_L) \quad (5.7)$$

where, $F(R_S, X_S)$ and $V_i(R_S, X_S, R_L, X_L)$ are noise figure and input VSWR functions given by Eqs. (5.1) and (5.2); F_{req} and V_{ireq} are the required noise and input VSWR

values, respectively. Thus, the cost (error) of this objective is evaluated by the following function in our work:

$$\varepsilon = e^{-\alpha G_T} + a\left|F - F_{req}\right| + b\left|V_i - V_{ireq}\right| \tag{5.8}$$

In the second part, the passive (Z_S, Z_L) termination pair is determined for the required gain $G_{T\min} \le G_T \le G_{T\max}$ constrained by the required noise, $F_{req} > F_{\min}$, and input VSWR, $V_{ireq} > 1$. The cost (error) function for this objective is as follows in our work:

$$\varepsilon = a\left|G_T - G_{Treq}\right| + b\left|F - F_{req}\right| + c\left|V_i - V_{ireq}\right| \tag{5.9}$$

In Eqs. (5.8) and (5.9), a, b, c are the weighting coefficients which can be chosen during the optimization process by trial.

5.3 Performance Characterization for a Transistor

It is chosen NE3512S02 NEC high-tech low noise transistor, which datasheet of the transistor is added to Appendix-1, to investigate with performance characterization. Transistor is examined for different DC bias, input reflection, maximum gain and required or minimum noise figure, see Figure 5.3 (G_T=G_{Tmax}, Freq=0.45 dB, Vireq=1.85), Figure 5.4 (V_{DS}=2 V, I_{DS}=20 mA, G_T=G_{Tmax} , F_{req}=0.45 dB), Figure 5.5 (F_{req}=F_{min}).

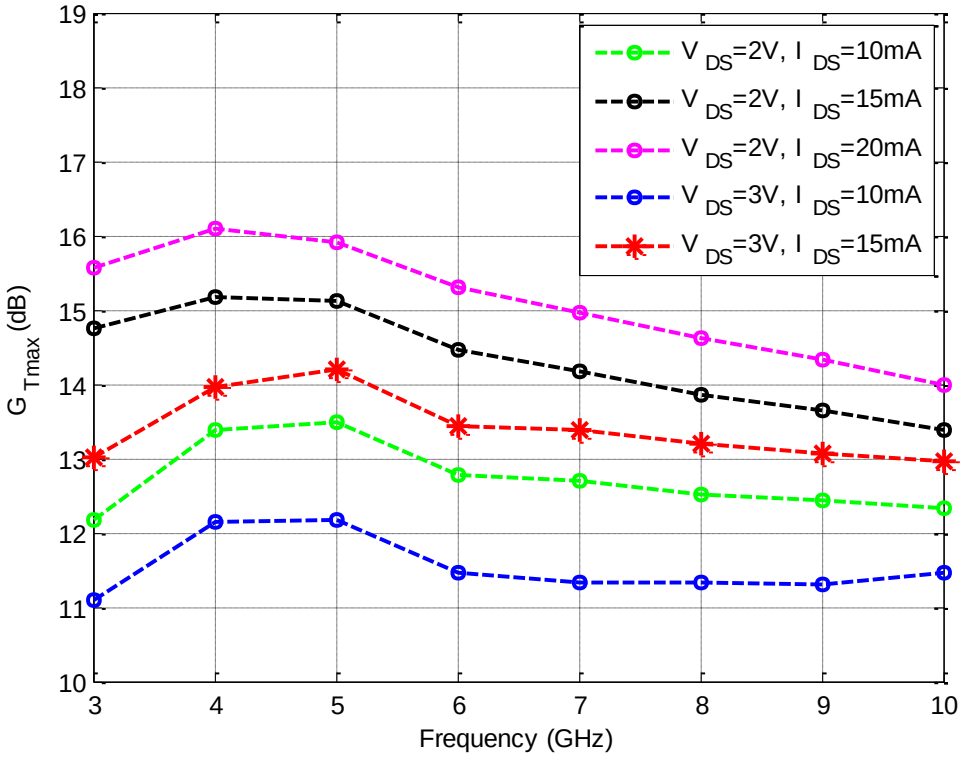

Figure 5. 3 Maximum gains for different DC bias conditions

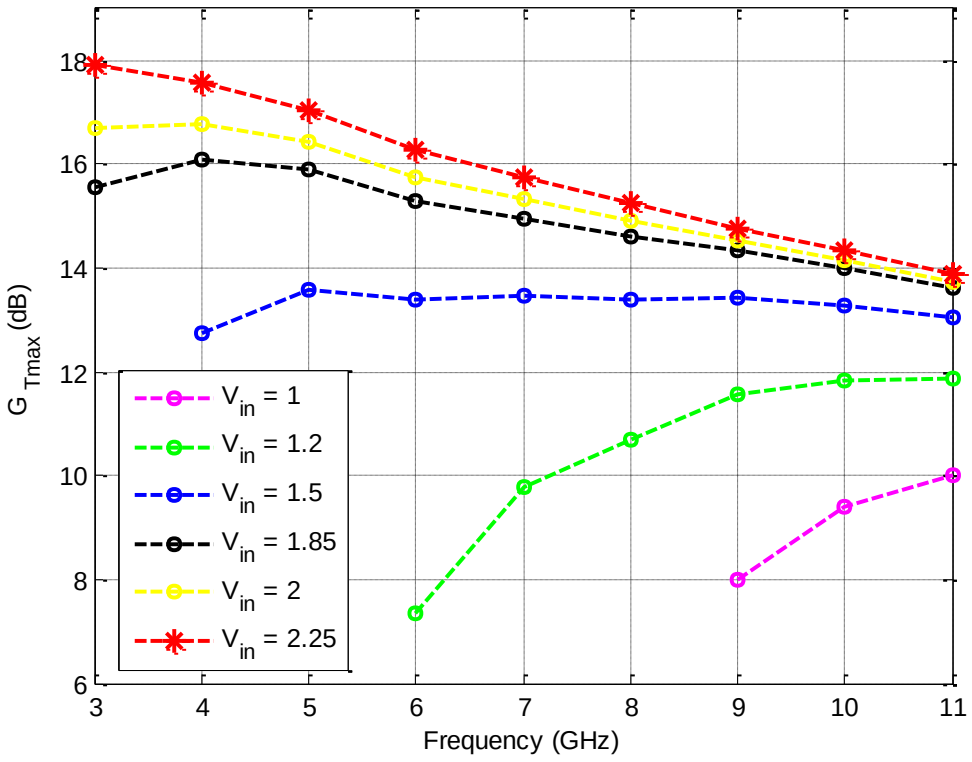

Figure 5. 4 Maximum gain for different input VSWR

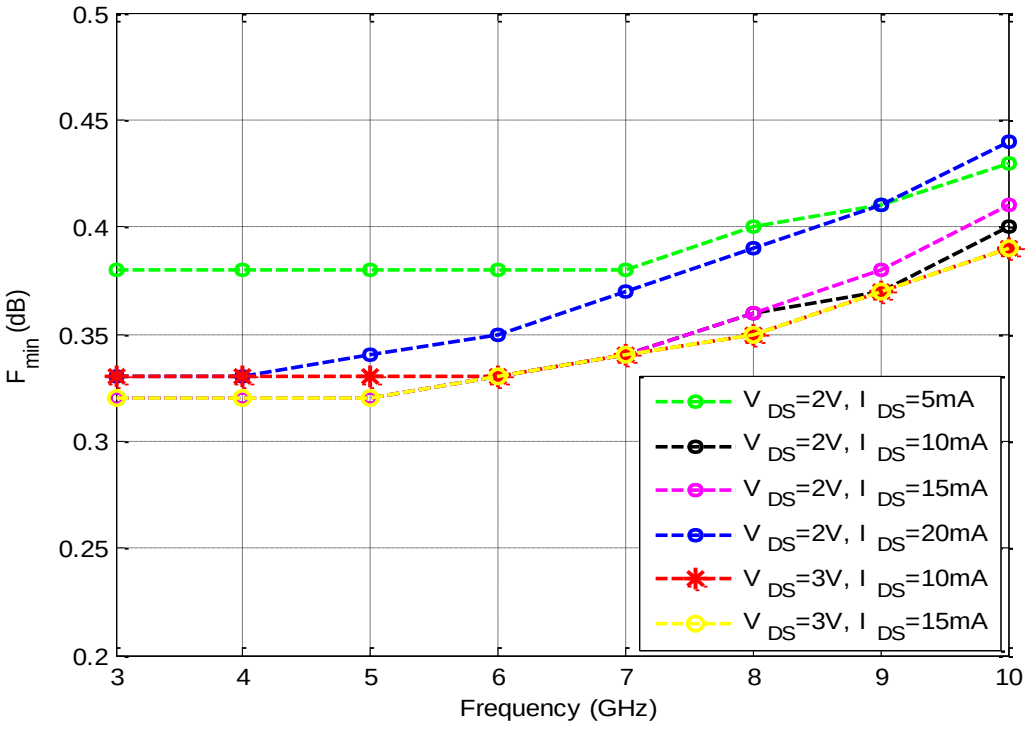

Figure 5. 5 Minimum noise figure for different DC bias conditions

CHAPTER 6

PARTICLE SWARM OPTIMIZATION

Particle swarm optimization, which has been developed with originating movements and intelligence of bird swarms by J. Kennedy and R.C. Eberhart, is population based stochastic optimization technique [19]. It was the result of many investigations about behaviors of bird swarms. It is an evolutionary algorithm capable of solving difficult multidimensional optimization problems in various fields. The PSO has gained an increasing popularity as an efficient alternative to Genetic Algorithm (GA) and Simulated Annealing (SA) in solving optimization design problems in antenna arrays. As an evolutionary algorithm, the PSO algorithm is similar to GA, it works with population of individuals randomly initialized and calculates fitness computation after each step, updates of the population based on the fitness value, and iterative algorithm stops when certain criteria are met [19].However, there is neither crossover nor mutation operations, in PSO to update the population, only the best particles are used.

PSO is designed to solve non-linear problems. It is used for continuous optimization problems and is useful to find a solution for multi-parameter and multi-variable optimization problems. For an N-dimensional problem, the position and velocity can be specified by M x N matrices, where M is the number of particles in the swarm. Each row of the position matrix represents a possible solution to the optimization problem. The velocity of each particle depends on the distance of the current position to the positions that resulted in good fitness values. To update the velocity matrix at each iteration, every particle should know its personal best and the global best position vectors. The personal best position of the ith particle is represented

as $P_{besti} = (P_{besti1}, P_{besti2}, .., P_{bestiN})$. The global best position vector defines the position in the solution space at which the best fitness value was achieved by all particles and is defined by $G_{besti} = (G_{best1}, G_{best2}, .., G_{bestN})$. Thus, all the information needed by the PSO algorithm is contained in X, P, P_{best} and G_{best}. The core of the PSO algorithm is the method by which these matrices are updated in every iteration of the algorithm. In our work, to achieve this, the velocity matrix is updated according to the following equation:

$$v_{mn}{}^{t} = wv_{mn}{}^{t} - 1 + c_1 U_{n1}{}^{t} \left(p_{mn}{}^{t} - x_{mn}{}^{t} - 1 \right) + c_2 U_{n2}{}^{t} \left(g_t - x_{mn}{}^{t} - 1 \right) \quad (6.1)$$

$$x_{k+1}^{i} = x_k^{i} + v_{k+1}^{i} \quad (6.2)$$

Where, the superscripts t and t1 refer to the time index of the current and the previous iterations, U_{n1} and U_{n2} are two uniformly distributed random numbers in the interval [0,1] and these random numbers are different for each of the n components of the particle's velocity vector. The parameters c_1 and c_2 are learning factors that usually $c_1 = c_2 = 2$. The parameter w is a number, called the "inertial weight," in the range [0,1], and its large values favor to global search, whereas the small values favor for local search. Inertial weight w is typically initialized to a value close to 1 and decreased linearly during the execution of the algorithm.

In Figure 6.1, flowchart of the PSO algorithm is presented. At the first stage, physical and convergence parameters of the algorithm are assigned. Position, velocity, personal best, and global best matrices are initialized randomly at the second stage. At each iteration, fitness function value is computed for each particle and these values define the each particle's personal best and global best value of the swarm. This convergence finishes when the target value is met or the algorithm reaches its maximum iteration number.

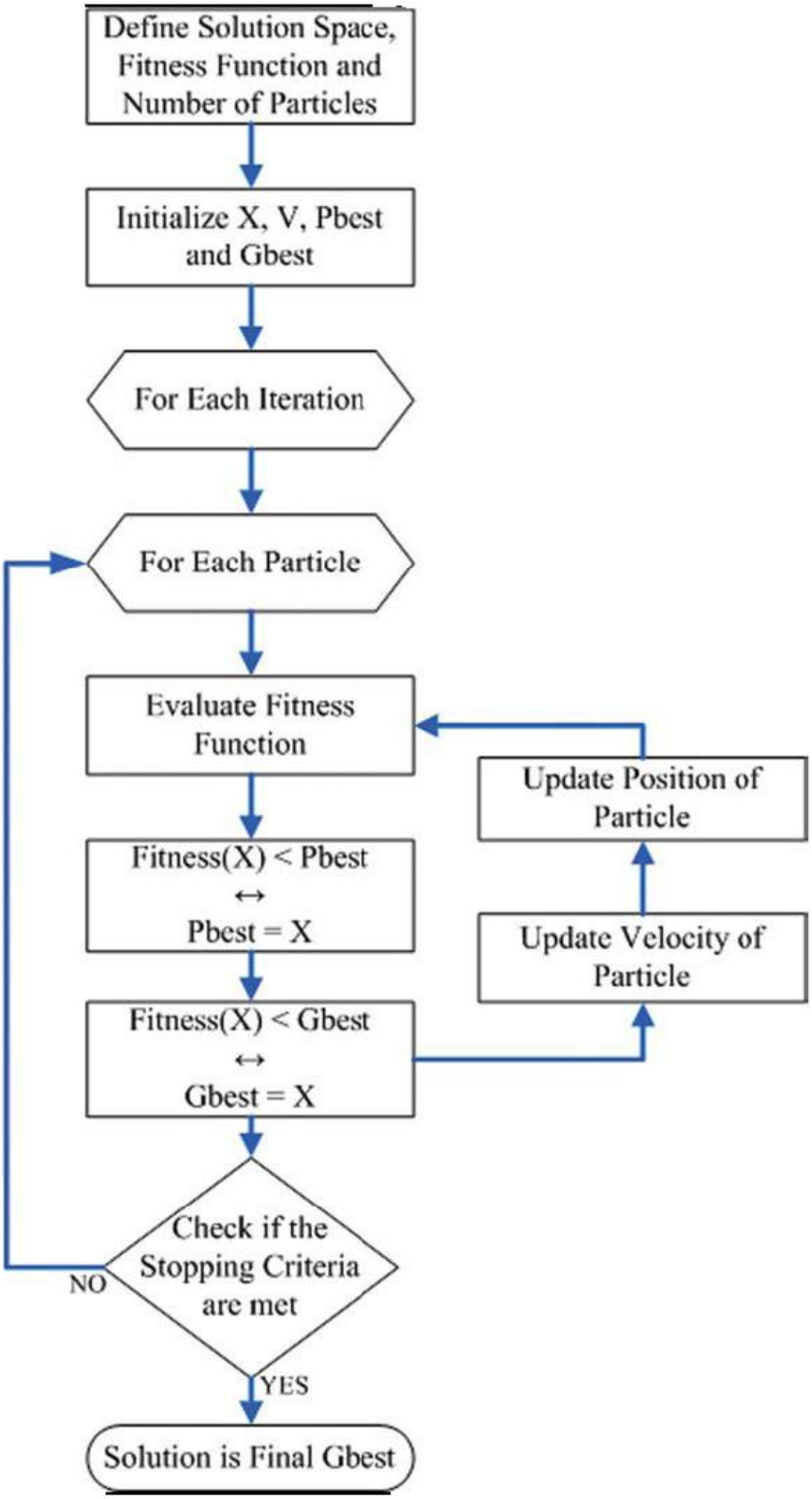

Figure 6. 1 PSO Algorithm

6.1 Advanced PSO

The most significant difference of advanced PSO is that algorithm searches the best position of previous self and adjacent particles. Average of P_{best} is calculated for each step and then, new particles is updated depends on this average and G_{best} values.

$$V_i^{k+1} = w.V_i^k + c_1.rand_1^k(p_i^{*k} - x_i^k) + c_2.rand_2^k.(gbest^k - x_i^k) \quad (6.3)$$

$$w_{new} = w\max - [(w\max - w\min * curriter / \max iter)] \quad (6.4)$$

Where w is weight, w should be chosen lower than 1 and it is decreased linearly at each iteration step. Inertial weight is decreased at each step with given equation 6.4. In PSO, inertial weight is used to balance the capability of local and global searching. If w has higher value, global searching will be easy, if it is lower, local searching will be easy. As a result of balancing operation, iteration number decreases. In these, each particle in swarm does not only benefit experience of best particles, but also other ones.

6.2 Repulsive PSO (RPSO)

RPSO is a global optimization algorithm. It is different version of PSO and it processes based on random evolutionary global optimizer classes. It usually works with repulsion of particles each other. This situation made particles prevent to local maxima. In other words, it is . In comparison with PSO, it is more effective to determinate global optimum points in more complex space. However, the pace of algorithm is slower than PSO.

$$v_{next} = \omega v + a\chi_1(-x + \hat{x}) + b\chi_2\omega(-x + \hat{y}) + c\chi_3\omega z \quad (6.5)$$

Where;

χ_1, χ_2, χ_3 : random numbers Є [0,1]

w: inertial weight

x: P_{best}

y: P_{best} value of the other particles chosen from swarm

z: random velocity vector

a,b,c:constant

6.3 Asynchronous PSO

In addition to principle of synchronic operation, there is asynchronous PSO algorithm. In this type of PSO, particle numbers are selected at lower value (between 1 and 5). After that, iterations are made without changes at updating equations. If optimization does not come through, maximum particle number will be an increased, and then iterations start again. This operation repeats till the optimization becomes succeed. Although the operation time rises, accomplishment with minimum particle number is an advantage.

CHAPTER 7

INPUT AND OUTPUT MATCING CIRCUIT OPTIMIZATION OF LOW NOISE ULTRAWIDE BAND AMPLIFIER USING 3-D SIMULATION BASED SVRM MICROSTRIP MODELING WITH PSO ALGORITHM

In the previous sections, it was stated that SVRM modeling of microstrip transmission line, performance characterization of a transistor and its matching impedances for required circumstances and PSO algorithm. In this section, matching networks for an UWB amplifier are optimized depends on an objective function and matching impedances for required conditions to obtain input and output matching circuit parameters. Matching networks are composed from T shaped microstrip lines. These microstrips are represented with high-accuracy and fast SVRM model in the optimization. The design procedure is given in Figure 7.1.

First of all, the parameters of microstrips are assigned by PSO to achieve the best solution and minimize objective function. Afterwards, SVRM generates the characteristic impedance and effective relative dielectric constant of each line depends on input parameters. ABCD parameter synthesizes the matching network with data from SVRM, and then IMN and OMN gain is calculated with respect to Z_S and Z_L. Finally, it is ended up with minimizing the objective function.

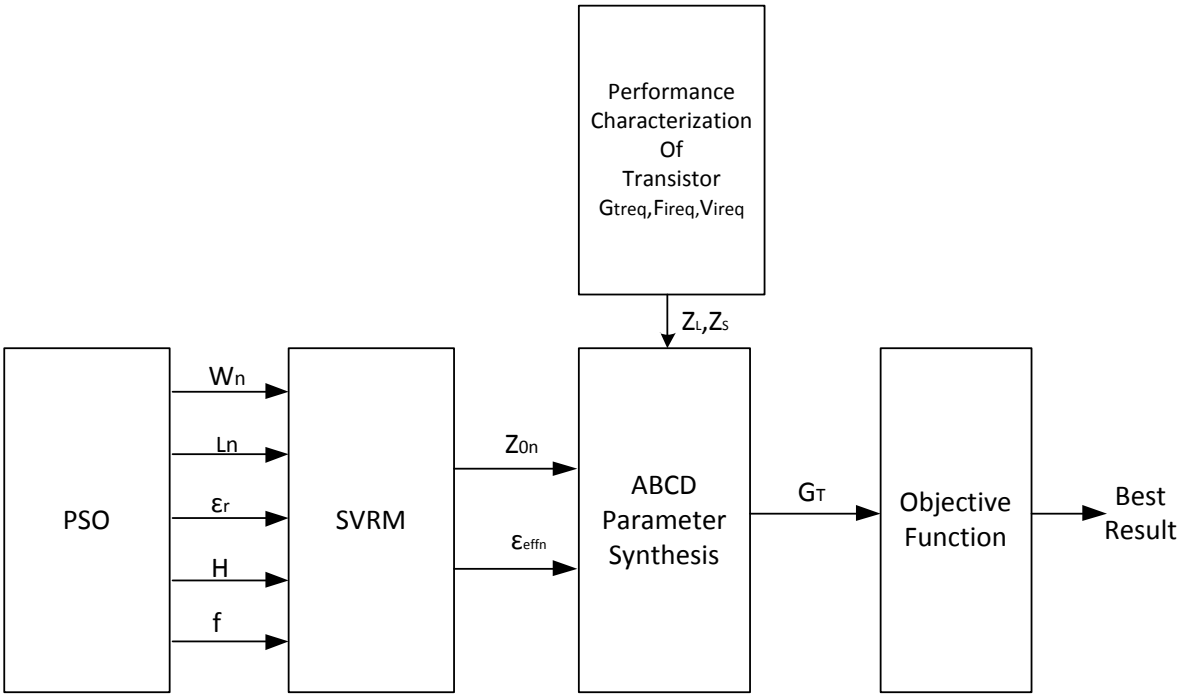

Figure 7. 1 Matching network optimization with SVRM and PSO

In PSO algorithm, the objective function is expressed as;

$$\varepsilon = \sum_i 1 - G_T(f_i) \tag{7.1}$$

where G_T is transducer gain of matching circuits (Eq. 5.3). Maximum gain for matching circuit is 1, because of its passive. With this objective function, it is aimed to maximize the gain of matching networks.

In the optimization, each microstrip line is described with its ABCD parameter because of easiness of solution. Total microstrip line number is 6, which 3 of them are for input and 3 of them are for output matching network. Learning machine number is 12 totally, namely 2 SVRM machine is used for each line. There are 12 optimization variables because each microstrip has 2 parameters as variant (W and L). ε_r and H are fixed. Input and output microstrip matching networks are given Figure 7.2 with their parameters. Besides, particle number is 20, c_1=c_2=2 and maximum iteration number is 250 for PSO algorithm.

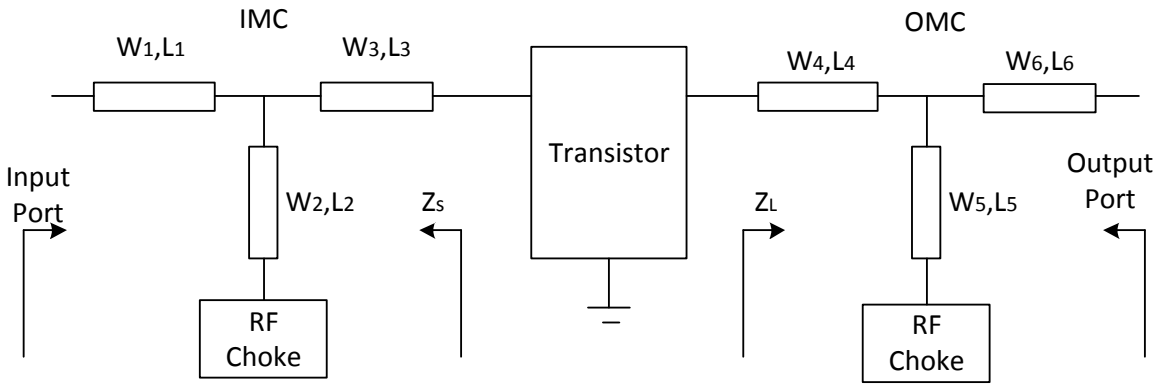

Figure 7. 2 Input and output matching network for the desired amplifier

It is purposed that minimum noise figure ($F_{ireq}=F_{min}$), maximum transducer gain ($G_{Treq}=G_{Tmax}$) and low VSWR ($V_{ireq}=1.85$) to build amplifier. NE3512S02 is chosen as transistor.

Designed amplifier operates at 2V 20mA DC bias and 3-8 GHz frequency band. To provide UWB DC bias and isolation, ADCH 80a+ RF choke is used. Input impedance for RF choke is given in Figure 7.3. The most significant specification for ADCH-80A+ is that its input impedance constant, even if it is added any component after it. More information is given in appendix-B. RO6002 is used as PCB substrate which has 2.94 relative dielectric permittivity (ε_r) and 0.762 mm height (H). In the optimization, limits of microstrip width (W) and length (L) are choosen minimum 0.25 mm, 0.25 mm and maximum 4.5 mm, 20 mm, respectively, because of technological constrations. Furthermore, 40 pF capacitors are used to block leakage of DC voltage to input and output ports at before IMN and after OMN.

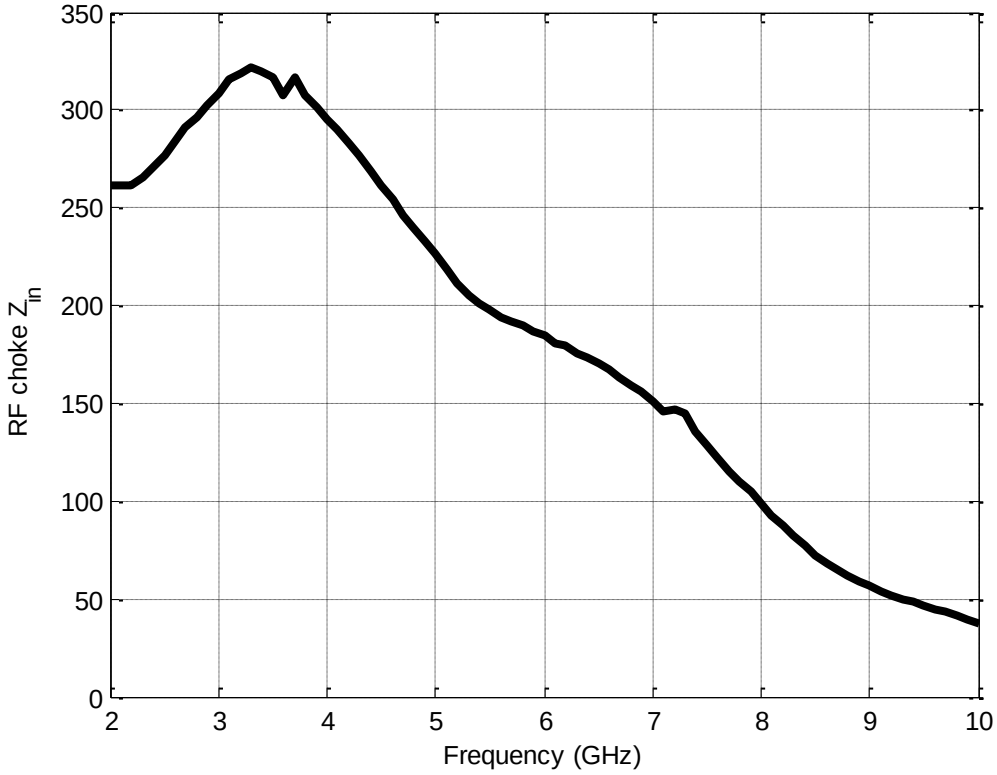

Figure 7. 3 Input impedance for ADCH-80a+

As a result of optimization, matching network parameters are acquired, they are given in Table 7.1. In Figure 7.4, it is given fitness value vs. iteration number graphic for optimization process.

Table 7. 1 Obtained parameters of matching networks

	1. Line	2. Line	3. Line	4. Line	5. Line	6. Line
W (mm)	2.4	0.25	0.25	0.75	0.25	3
L (mm)	4.25	14.5	2.5	13	6.5	15.75
Z_0 (ohm)	42.96	124.3	124.3	82.8	124.3	36.8

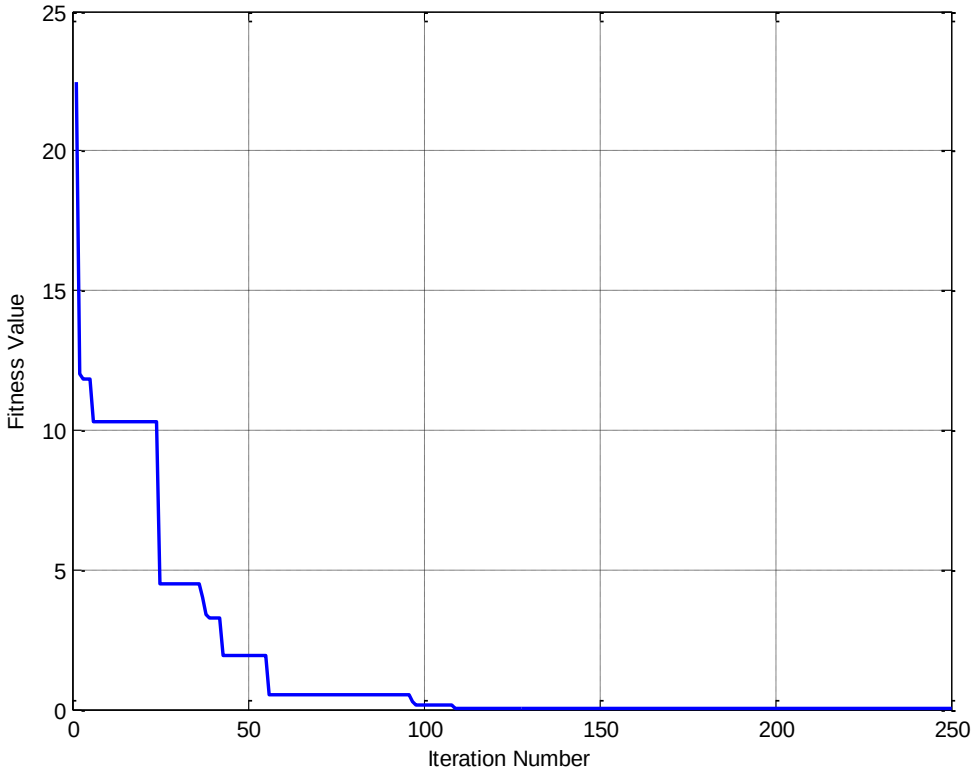

Figure 7. 4 Fitness value corresponding to iteration number

7.1 Practical Design and Comparative Results

It was obtained that performance characterization of NE3512S02 transistor and input and output matching circuit parameters low noise ultra wide-band amplifier which is built with this transistor. According to acquiring parameters, the amplifier circuit is fabricated in our lab with LPKF S63 circuit print device, see Figure 7.5. Afterwards, input-output VSWR and gain of the amplifier are measured with vector network analyzer; it is showed in Figure 7.6.

Figure 7. 5 LPKF device

Figure 7. 6 Network analyzer

Printed and measured amplifier circuit is presented in Figure 7.7. The measurement results are compared with performance characterization (PerCHar), PSO and simulation results. Micorwave office AWRDE is used as simulation program [20]. The comparative results are presented in Figure 7.8-12.

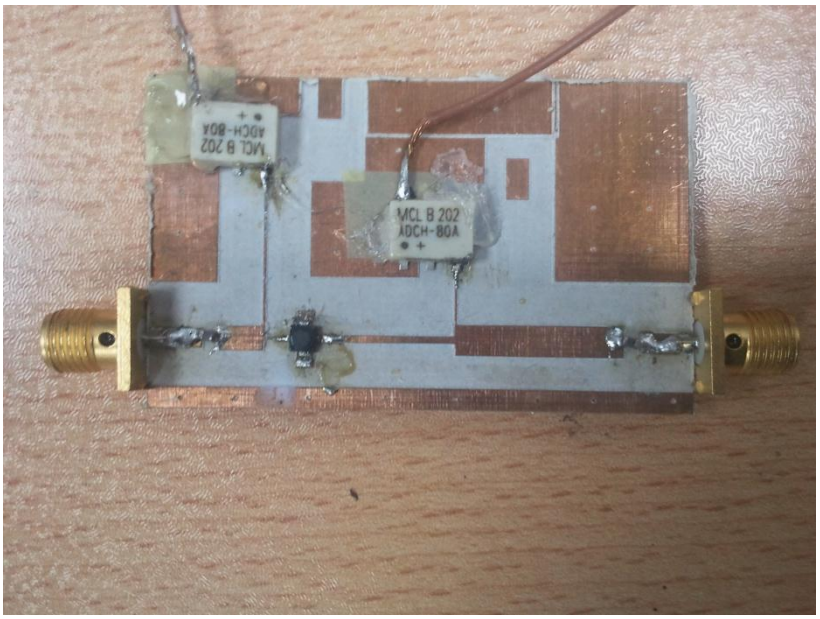

Figure 7. 7 Fabricated UWB low noise amplifier

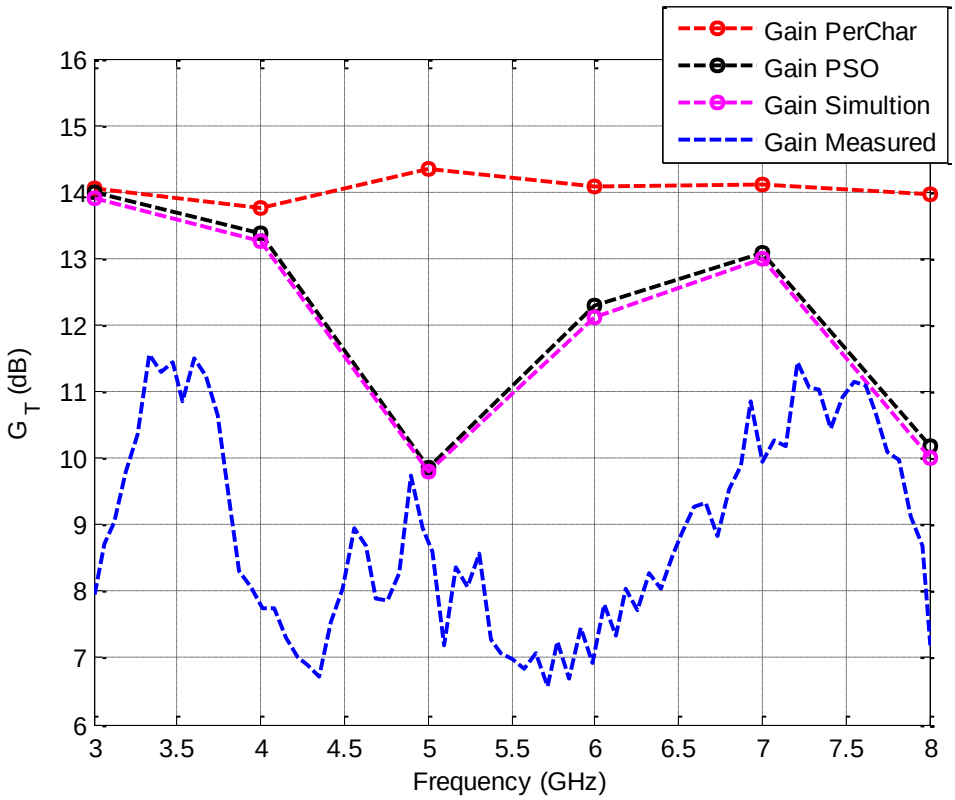

Figure 7. 8 Transducer gain of designed amplifier

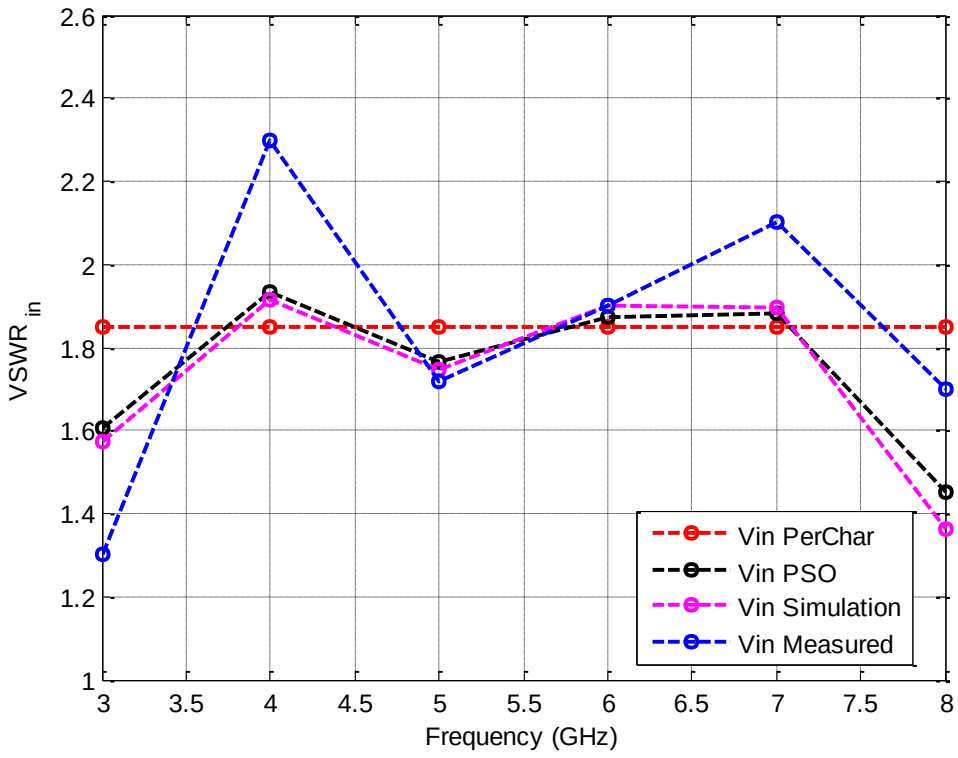

Figure 7. 9 Input VSWR of designed amplifier

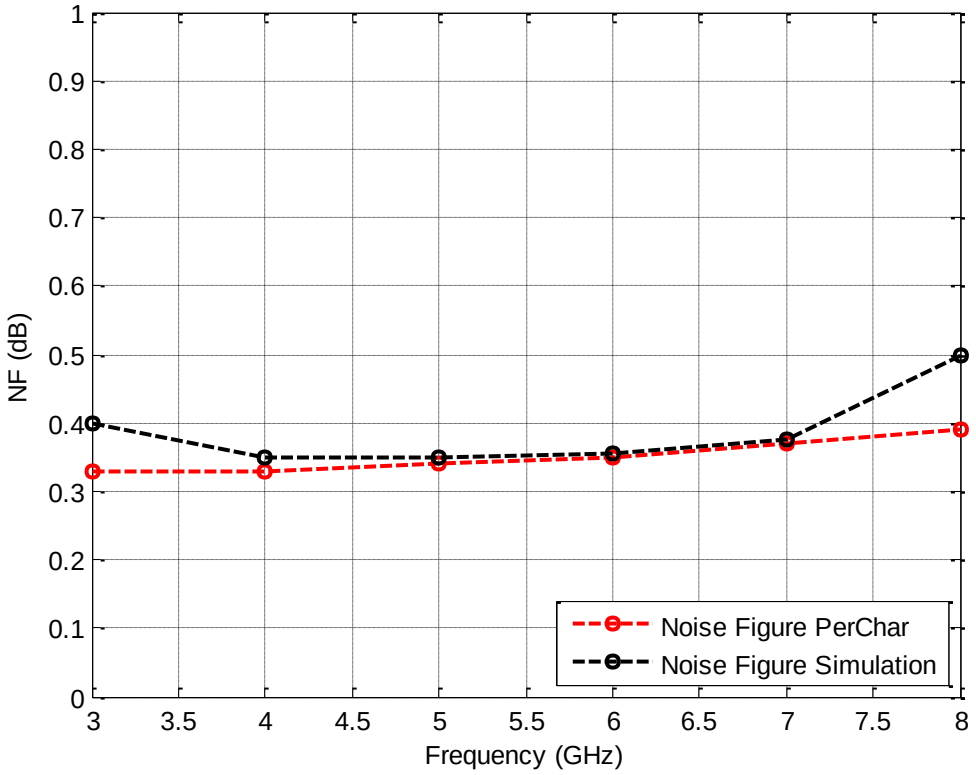

Figure 7. 10 Noise figure of amplifier

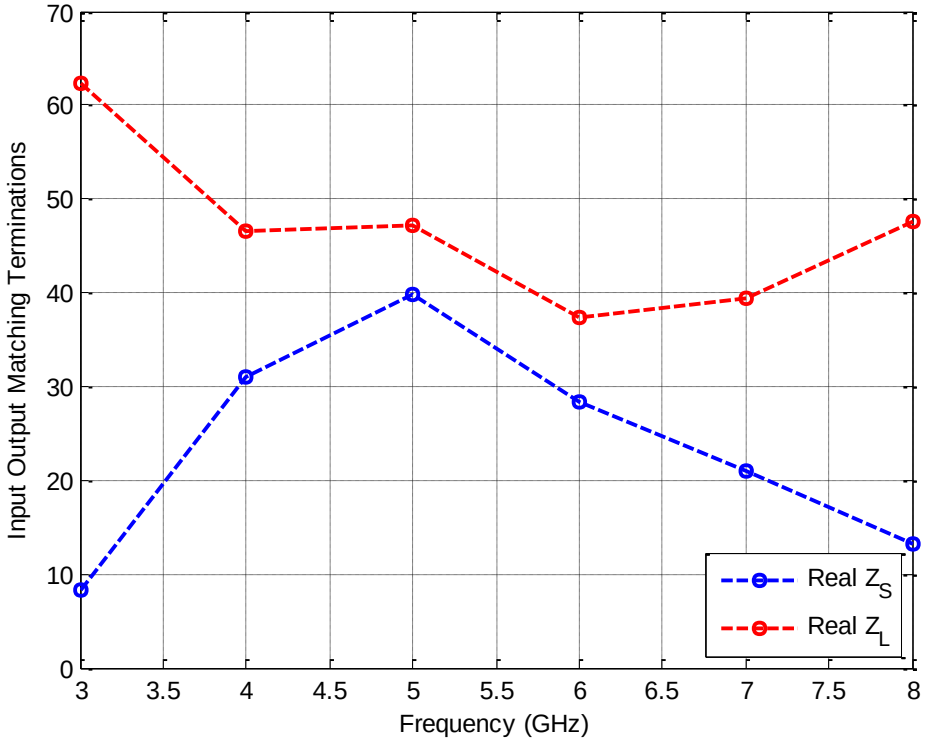

Figure 7. 11 Real input output matching terminations (ZS,ZL) for V_{ireq}=1.85, G_{Tmax}, F_{min}

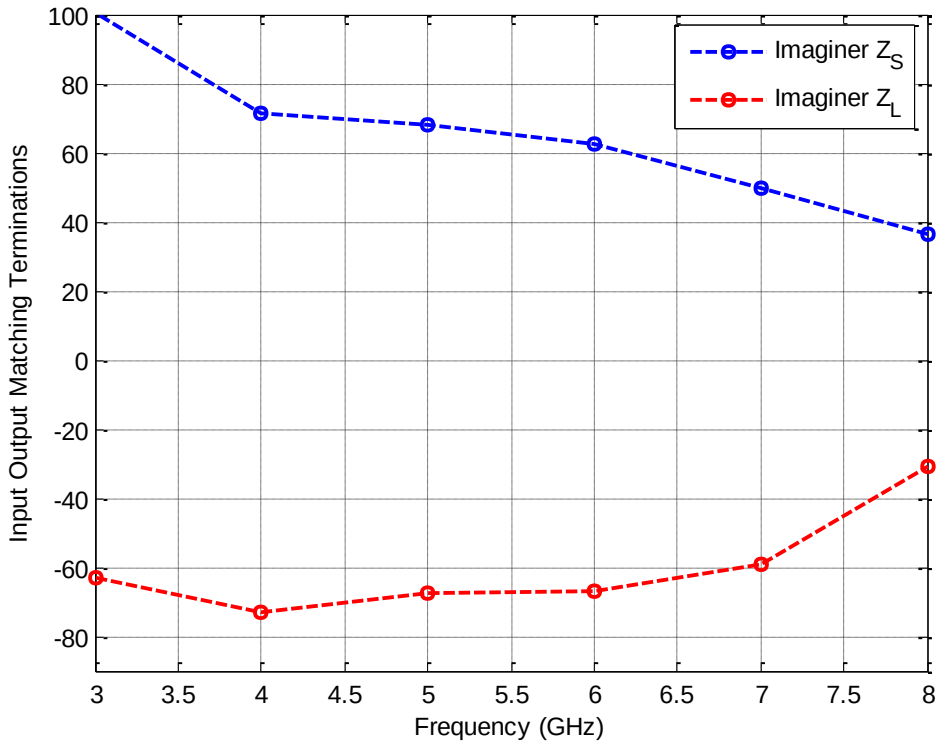

Figure 7. 12 Imaginer input output matching terminations (ZS,ZL) for V_{ireq}=1.85, G_{Tmax}, and F_{min}

The measurement results for input and output reflection and gain is presented in Figure 7.13-14;

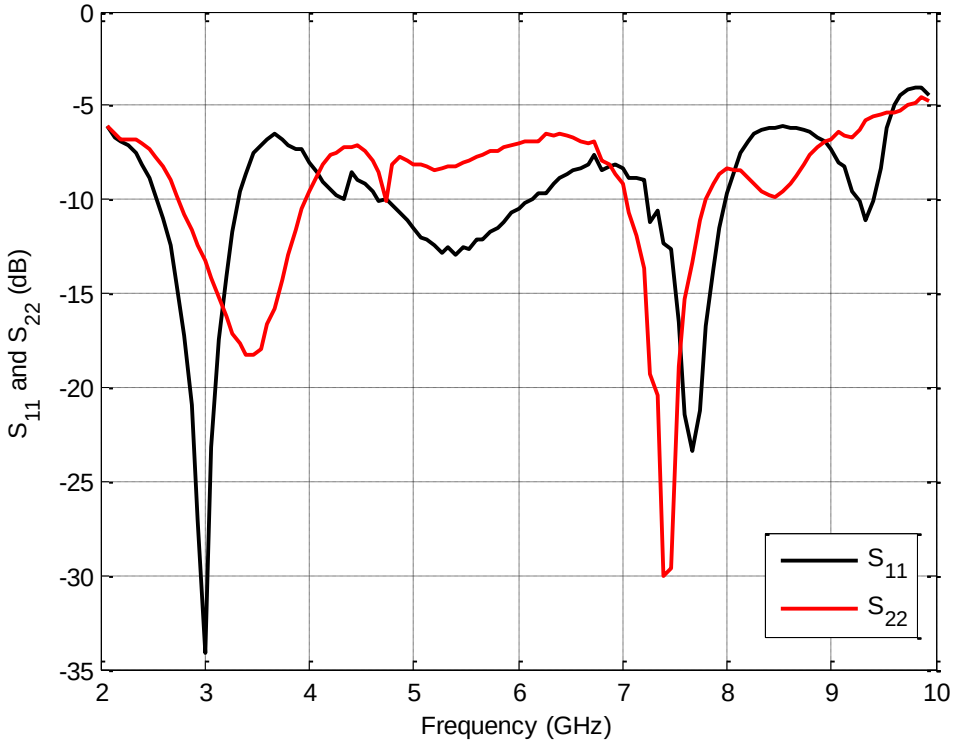

Figure 7. 13 Measured input and output reflection (S11 and S22)

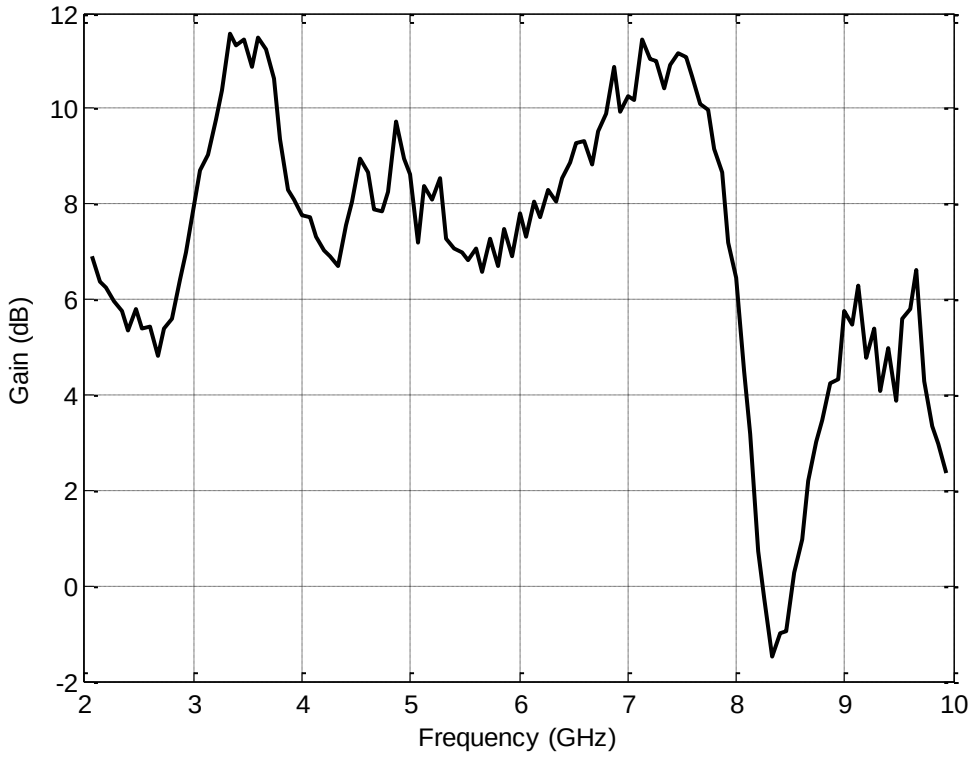

Figure 7. 14 Measured S21 of amplifier

7.2 Conclusion

Performance characterization for NE3512S02 transistor is performed to obtain UWB and low noise amplifier. As a result of characterization Z_S, Z_L matching terminations are acquired for certain conditions of V_{ireq}, F_{ireq} and G_{Treq}. According to desired VSWR, gain, noise conditions, input and output matching network parameters are optimized with PSO depends on the matching termination impedances. PSO, performance characterization and SVRM works together to get the purposed conditions V_{ireq}=1.85, F_{ireq}=F_{min}, G_{Treq}=G_{Tmax}. With obtained parameters, designed amplifier is printed on RO6002 substrate and measured. Then, PSO, performance characterization, simulation and measurement results are compared with each other. In accordance with measurement results, the designed amplifier operates at 3-8 GHz frequency band. The dimension of the circuit is 6.5 cm x 3 cm. Moreover, its average gain is 10 dB at all-over operational band and its input and output reflection is beneath of -8 dB. Noise figure was not measured, according to simulation programs and performance characterization it is about 0.35 dB (F_{min}). As can be seen in comparative results, measured gain level is a bit less than PSO.

CHAPTER 8

CONCLUSION & SUGGESTIONS

Microwave technology is expeditiously improving day by day. This improvements due to high-accuracy 3D computer aided design. Although 3D simulations are so accurate, there is significant disadvantage like slowness. In order to solve this problem, one of the important methods is learning machines. Nonlinear learning machines are widely employed as the fast and flexible machines in the generalization of the highly nonlinear input-output discrete mapping relations in the microwave modeling. In this thesis, Support Vector Regression machine is used to model microstrip transmission line. Afterward, obtained fast and accurate SVRM model is simultaneously operated with PSO and performance characterization to design a microwave amplifier system. These SVRM model and its using with PSO to design an amplifier could be said as contribution to the literature. Performed investigations and designs could be summed up as follows;

1. Microstrip transmission line is modeled with SVRM learning machine. Coarse and fine model of microstrip line is obtained. The SVRM model of microstrip line is high-accuracy like 3D SONNET EM simulation programs and fast like empirical formulations. SVRM model is 400 times faster than SONNET simulator.
2. Performance characterization for NE3512S02 transistor is performed to obtain UWB and low noise amplifier. As a result of characterization Z_S, Z_L matching terminations are acquired for certain conditions.
3. According to desired VSWR, gain, noise conditions, input and output matching network parameters are optimized with PSO depends on the matching termination

impedances. PSO, performance characterization and SVRM are combined to get the purposed conditions.

4. With obtained parameters, designed amplifier is printed and measured. Then, PSO, performance characterization, simulation and measurement results are compared with each other. As can be seen in comparative results, measured gain level is a bit less than PSO. Besides, input VSWR level is close to desired targets. Therefore, it is understood that PSO, performance characterization and SVRM work together successfully to design an amplifier.

REFERENCES

[1] Zhang, Q. J. and Gupta, K. C., (2000). Neural Networks for RF and Microwave Design, Artech House, Norwood, MA.

[2] Vapnik, V., (1995). The Nature of Statistical Learning Theory, Springer - Verlag, New York.

[3] Bermani, E., Boni, A., Kerhet, A. and Massa, A., (2005). "Kernels evaluation of SVM based estimatiors for inverse scattering problems," Progress In Electromagnetics Research, 53: 167–188.

[4] Güneş, F., Tokan, N. T. and Gürgen, F., (2007). "Signal-noise support vector model of a microwave transistor," Int. J. RF and Microwave CAE, 17: 404–415.

[5] Shawe-Taylor, J. and Cristianini, N., (2000). An Introduction to Support Vector Machines and Other Kernel-Based Learning Methods, Cambridge University Press.

[6] Watson, P. M., Gupta, K. C., and Mahajan, R. L., (1999). "Applications of knowledge-based artificial neural network modeling to microwave components," Int. J. RF Microwave Computer-aided Eng., 9: 254–260.

[7] Jargon, J. A., Gupta, K. C. and DeGroot, D. C., (2002). "Applications of artificial neural networks to RF and microwave measurements," Int. J. RF Microwave Computer-aided Eng., 12: 3–24.

[8] Bandler, J. W., Ismail, M. A., Rayas-Sanchez, J. E. and Zhang, Q. J., (1999). "Neuromodeling of microwave circuits exploiting space-mapping technology," IEEE Trans. Microwave Theory Tech., 47: 2417–2427.

[9] Bakr, M. H., Bandler, J. W., Ismail, M. A., Rayas-Sanchez, J. E. and Zhang, Q. J., (2000). "Neural space-mapping optimization for EMbased design," IEEE Trans. Microwave Theory Tech., 48: 2307–2315.

[10] Devabhaktuni, V. K., Yagoub, M. C. E. and Zhang, Q. J., (2001). "A robust algorithm for automatic development of neural network models for microwave applications," IEEE Trans. Microwave Theory Tech., 49: 2282–2291.

[11] Bandler, J. W., Rayas-Sanchez, J. E. and Zhang, Q. J., (2002). “Yielddriven electromagnetic optimization via space mapping-based neuromodels,” Int. J. RF Microwave Computer-aided Eng., 12: 79–89.

[12] Devabhaktuni, V. K., Chattaraj, B., Yagoub, M. C. E. and Zhang, Q. J., (2003).“Advanced microwave modeling framework exploiting automatic model generation, knowledge neural networks, and space mapping,” IEEE Trans. Microwave Theory Tech., 51(7): 1822–1833.

[13] Güneş F., Tokan N.T., Gürgen F., (2010). “A knowledge-based support vector synthesis of the transmission lines for use in microwave integrated circuits”, Expert Systems with Applications, 37(4): 3302-3309,

[14] SONNET 3-D Planar High Frequency Electromagnetic Software, http://www.sonnetsoftware.com/products/sonnet-suites, 05/2012

[15] Güneş, F., Güneş, M. and Fidan, M.,(1994). “Performance Characterisation of a Microwave Transistor”, IEE Proceedings-Circuits, Devices and Systems, 141(5): 337-344.

[16] Güneş, F. and Çetiner, B. A., (1998). “A Novel Smith Chart Formulation of Performance Characterisation for a Microwave Transistor”, IEE Proceedings - Circuits Devices and Systems, 145(6): 419–428.

[17] Güneş, F., Torpi, H. and Gürgen, F., (1998). “A multidimensional signal-noise neural network model for microwave transistors”, IEE Proc Circ Devices Syst 145: 111–117.

[18] Güneş, F., Özkaya, U. and Demirel, S., “Performance datasheets for use in the low-noise amplifier design”, Int. J RF Microwave Comput-Aided Eng, in press.

[19] Kennedy, J. and Eberhart, R.C., (1995). Particle swarm optimization, In Proceedings of the IEEE Conference Neural Networks IV, Piscataway, NJ.

[20] Microwave Office AWRDE http://web.awrcorp.com/Usa/Products/Microwave–Office, 05/2012

NE3512S02 NEC TRANSISTOR DATASHEET

CEL

HETERO JUNCTION FIELD EFFECT TRANSISTOR
NE3512S02

C TO Ku BAND SUPER LOW NOISE AMPLIFIER
N-CHANNEL HJ-FET

FEATURES

- Super low noise figure and high associated gain
  NF = 0.35 dB TYP., G_a = 13.5 dB TYP. @ f = 12 GHz
- Micro-X plastic (S02) package

APPLICATIONS

- C to Ku-band DBS LNB
- Other C to Ku-band communication systems

ORDERING INFORMATION

Part Number	Order Number	Package	Quantity	Marking	Supplying Form
NE3512S02-T1C	NE3512S02-T1C-A	S02 (Pb-Free)	2 kpcs/reel	C	• 8 mm wide embossed taping • Pin 4 (Gate) faces the perforation side of the tape
NE3512S02-T1D	NE3512S02-T1D-A		10 kpcs/reel		

Remark To order evaluation samples, contact your nearby sales office.
Part number for sample order: NE3512S02

ABSOLUTE MAXIMUM RATINGS (T_A = +25°C)

Parameter	Symbol	Ratings	Unit
Drain to Source Voltage	V_{DS}	4	V
Gate to Source Voltage	V_{GS}	–3	V
Drain Current	I_D	I_{DSS}	mA
Gate Current	I_G	100	μA
Total Power Dissipation	P_{tot} Note	165	mW
Channel Temperature	T_{ch}	+125	°C
Storage Temperature	T_{stg}	–65 to +125	°C

Note Mounted on 1.08 cm^2 × 1.0 mm (t) glass epoxy PCB

RECOMMENDED OPERATING CONDITIONS (T_A = +25°C)

Parameter	Symbol	MIN.	TYP.	MAX.	Unit
Drain to Source Voltage	V_{DS}	1	2	3	V
Drain Current	I_D	5	10	15	mA
Input Power	P_{in}	–	–	0	dBm

ELECTRICAL CHARACTERISTICS (T_A = +25°C, unless otherwise specified)

Parameter	Symbol	Test Conditions	MIN.	TYP.	MAX.	Unit
Gate to Source Leak Current	I_{GSO}	V_{GS} = –3 V	–	0.5	10	μA
Saturated Drain Current	I_{DSS}	V_{DS} = 2 V, V_{GS} = 0 V	15	40	70	mA
Gate to Source Cutoff Voltage	$V_{GS(off)}$	V_{DS} = 2 V, I_D = 100 μA	–0.2	–0.7	–2.0	V
Transconductance	g_m	V_{DS} = 2 V, I_D = 10 mA	40	55	–	mS
Noise Figure	NF	V_{DS} = 2 V, I_D = 10 mA, f = 12 GHz	–	0.35	0.5	dB
Associated Gain	G_a		12.5	13.5	–	dB

TYPICAL CHARACTERISTICS (T_A = +25°C, unless otherwise specified)

TOTAL POWER DISSIPATION vs. AMBIENT TEMPERATURE

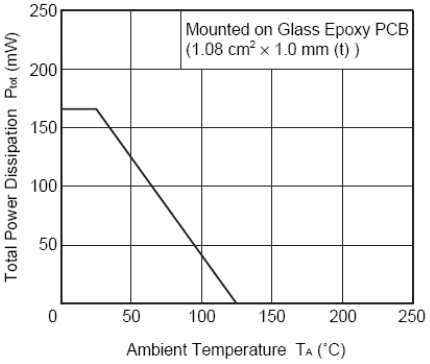

DRAIN CURRENT vs. DRAIN TO SOURCE VOLTAGE

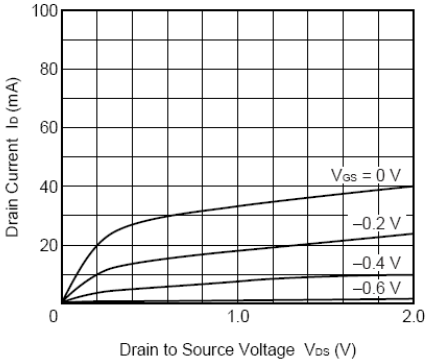

DRAIN CURRENT vs. GATE TO SOURCE VOLTAGE

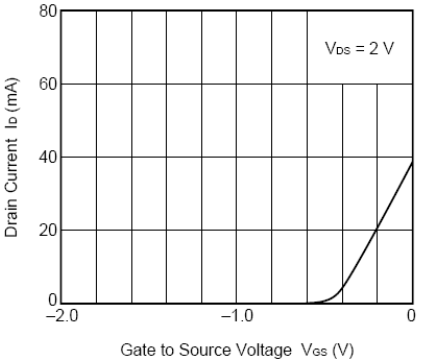

MINIMUM NOISE FIGURE, ASSOCIATED GAIN vs. FREQUENCY

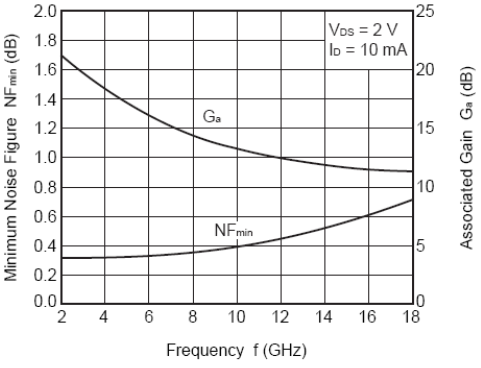

MINIMUM NOISE FIGURE, ASSOCIATED GAIN vs. DRAIN CURRENT

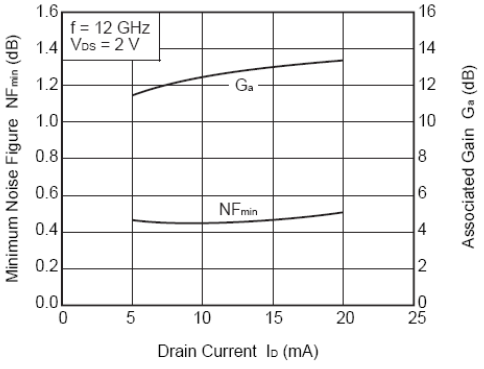

Remark The graphs indicate nominal characteristics.

ADCH-80A+ RF CHOKE DATASHEET

Very Wideband

RF Choke

50Ω 50 to 10000 MHz

ADCH-80A+
ADCH-80A

CASE STYLE: CD542
PRICE: $2.75 ea. QTY. (10-49)

+ RoHS compliant in accordance with EU Directive (2002/95/EC)

The +Suffix identifies RoHS Compliance. See our web site for RoHS Compliance methodologies and qualifications.

Maximum Ratings

Operating Temperature	-40°C to 85°C
Storage Temperature	-55°C to 100°C
DC Current	250 mA

Permanent damage may occur if any of these limits are exceeded.

Pin Connections

RF-IN & DC	6
DC	3
NOT USED	1,2,4,5

Features

- low parasitic capacitance 0.1 pf typ.
- effective parallel resistance, Rch 800 ohm typ.
- aqueous washable
- protected by US Patent, 6,133,525

Applications

- biasing amplifiers
- biasing of laser diodes

Outline Drawing

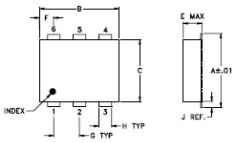

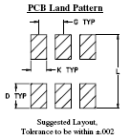

Outline Dimensions (inch / mm)

A	B	C	D	E	F	G
.272	.310	.220	.100	.112	.055	.100
6.91	7.87	5.59	2.54	2.84	1.40	2.54

H	J	K	L	wt
.030	.026	.065	.300	grams
0.76	0.66	1.65	7.62	0.20

Demo Board MCL P/N: TB-113
Suggested PCB Layout (PL-026)

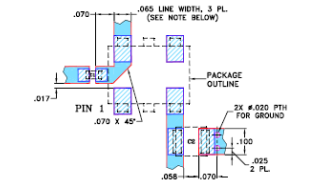

CAPASITORS: C1: 6800 pF, 0603 SIZE; C2: 1.0 uF, 1311 SIZE.
NOTES: 1. TRACE WIDTH IS SHOWN FOR ROGERS RO4350B WITH DIELECTRIC THICKNESS .030" ± .002"; COPPER: 1/2 OZ. EACH SIDE. FOR OTHER MATERIALS TRACE WIDTH MAY NEED TO BE MODIFIED.
2. BOTTOM SIDE OF THE PCB IS CONTINUOUS GROUND PLANE.

DENOTES PCB COPPER LAYOUT WITH SMOBC (SOLDER MASK OVER BARE COPPER)

DENOTES COPPER LAND PATTERN FREE OF SOLDER MASK

Electrical Specifications

FREQ. RANGE (MHz)	INSERTION LOSS* (dB)		VSWR* (:1)		DC CURRENT (mA)	INDUCTANCE (µH) Typ.		
	Typ.	Max.	Typ.	Max.	Max.	@ 0mA	@ 50mA	@ 100mA
50-8000	0.3	1.0	1.1	1.35	100	7.0	1.8	1.0
50-10000	0.3	2.0	1.1	1.6	100	7.0	1.8	1.0

*tested with circuit shown below, Zo=50 ohms

Typical Performance Data

FREQUENCY (MHz)	INSERTION LOSS (dB)	VSWR (:1)
50.00	0.38	1.12
100.00	0.32	1.09
300.00	0.31	1.08
500.00	0.32	1.08
1000.00	0.27	1.09
2000.40	0.44	1.10
3000.90	0.53	1.12
3900.00	0.42	1.15
4500.00	0.51	1.10
5400.00	0.55	1.14
6000.00	0.65	1.12
7199.80	0.51	1.15
8500.00	0.31	1.12
9500.20	0.81	1.17
10000.30	0.42	1.07

ADCH-80A
INSERTION LOSS

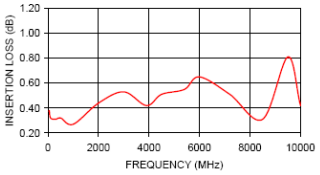

ADCH-80A
VSWR

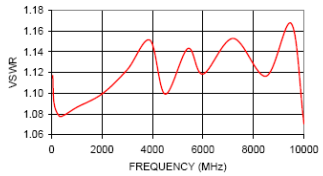

electrical schematic

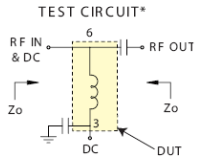

Mini-Circuits®
ISO 9001 ISO 14001 AS9100 CERTIFIED

For detailed performance specs & shopping online see web site

P.O. Box 350166, Brooklyn, New York 11235-0003 (718) 934-4500 Fax (718) 332-4661 *The Design Engineers Search Engine* Provides ACTUAL Data Instantly at minicircuits.com

IF/RF MICROWAVE COMPONENTS

Notes: 1. Performance and quality attributes and conditions not expressly stated in this specification sheet are intended to be excluded and do not form a part of this specification sheet. 2. Electrical specifications and performance data contained herein are based on Mini-Circuit's applicable established test performance criteria and measurement instructions. 3. The parts covered by this specification sheet are subject to Mini-Circuits standard limited warranty and terms and conditions (collectively, "Standard Terms"); Purchasers of this part are entitled to the rights and benefits contained therein. For a full statement of the Standard Terms and the exclusive rights and remedies thereunder, please visit Mini-Circuits' website at www.minicircuits.com/MCLStore/terms.jsp.

REV. C
M102713
ED-8059
ADCH-80A
DJ/TD/CP/AM
070530

AUTOBIOGRAPHY

PERSONAL INFORMATION

Name-Surname :Ahmet Kenan KESKİN

Birthplace and Date :Samsun/29.10.2012

Foreign Language :English

E-mail :kkeskin@yildiz.edu.tr

EDUCATIONAL STATUS

Degree	Branch	School/University	Graduate Year
Undergraduate	Electronics and Communications Engineering	Yildiz Technical University	2010

WORK EXPERIENCES

Year	Firm	Assignment
2011	Yildiz Technical University	Research Assistant

Conference Paper

1. Turk, A. S. and Keskin A. K., (2011). “Vivaldi shaped TEM horn fed ridged horn antenna design for UWB GPR systems”, Advanced Ground Penetrating Radar (IWAGPR) 6th International Workshop on, Germany

2. Keskin, A. K., Partal, H. P. and Arvas, E., (2011). “Wi-Fi frekans Bandında Çalışan LNA Tasarımı”, ASELSAN Haberleşme Çalıştayı, Ankara

Project

1. Avea Indoor Localization Project for Shopping Malls

Awards

1. The Scientific and Technological Research Council of Turkey (TUBITAK) Scholarship for Master Students